Introduction to radio astronomy
Lectures 5 and 6

Miroslav Bárta
barta@asu.cas.cz

EUROPEAN ARC
ALMA Regional Centre || Czech

Astronomical Institute
of the Czech Academy
of Sciences

Outline – Lectures 5 and 6

- Methods of radio astronomy – a quick overview
  - Radiometry, polarimetry,
  - SD imaging
  - „Active“ radioastronomy – radar sounding
  - Radio spectroscopy
  - Interferometry overview – sparse phased arrays, aperture synthesis
- Intro to (solar) radio spectroscopy
  - Meaning of radio spectra
  - Examples at metric wavelengths
  - Decimeter emission – flare related bursts
  - Calibration of spectroscopic data
  - Non-solar applications
- Intro to interferometry/aperture synthesis
  - Basic principles of Fourier imaging
  - From complex visibilities to „real“ image

All lectures to be found at: http://wave.asu.cas.cz/barta/lectures/radioastronomy

Brief overview/comparison of all methods

Methods of radio astronomy

Radiometry

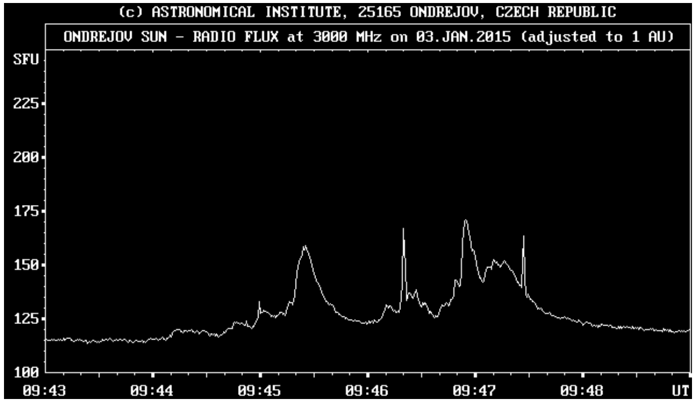

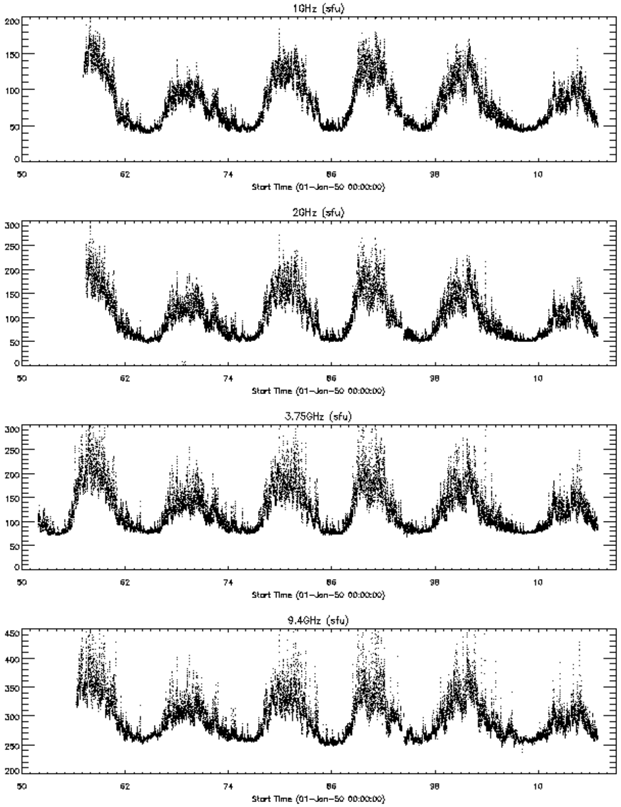

Result: A light curve
Pros: Good time resolution
Cons: No spatial, spectral nor pol. information

Methods of radio astronomy

Radiometry

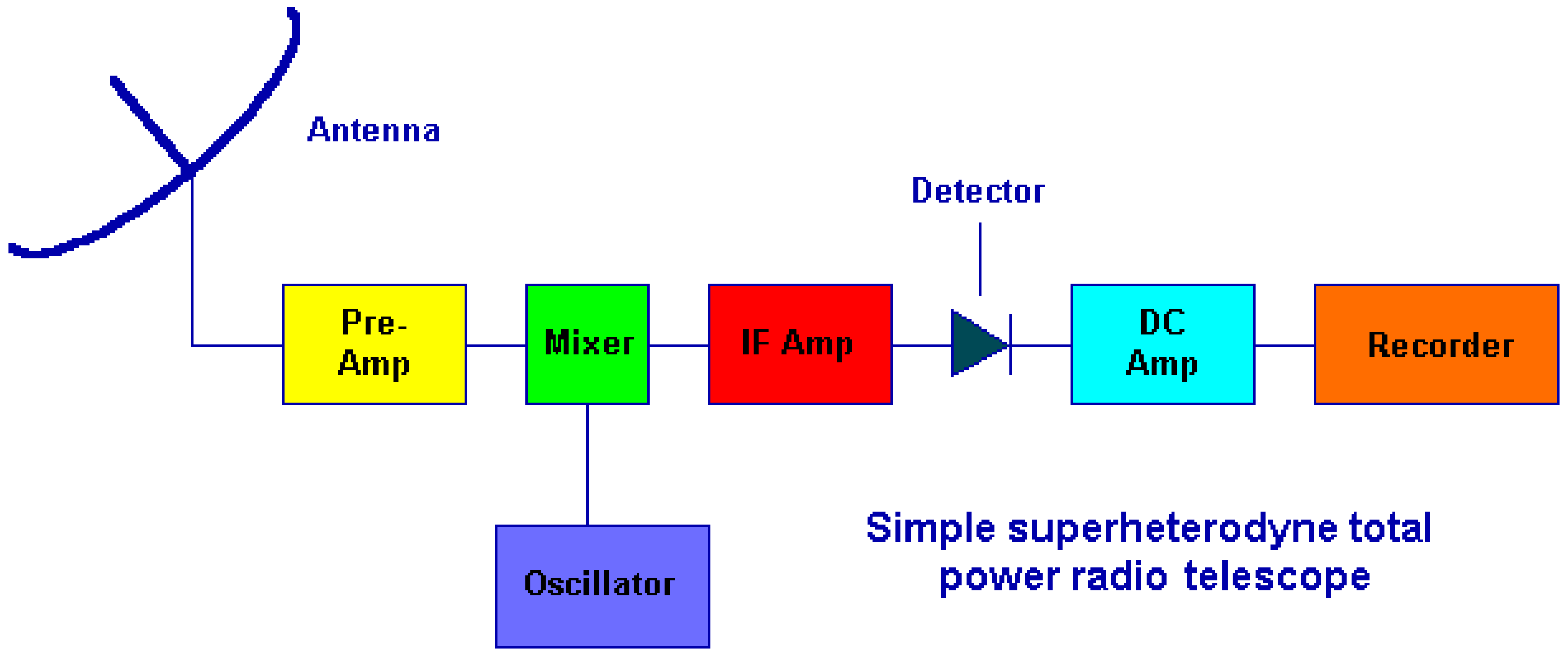

Methods of radio astronomy

Radio polarimetry

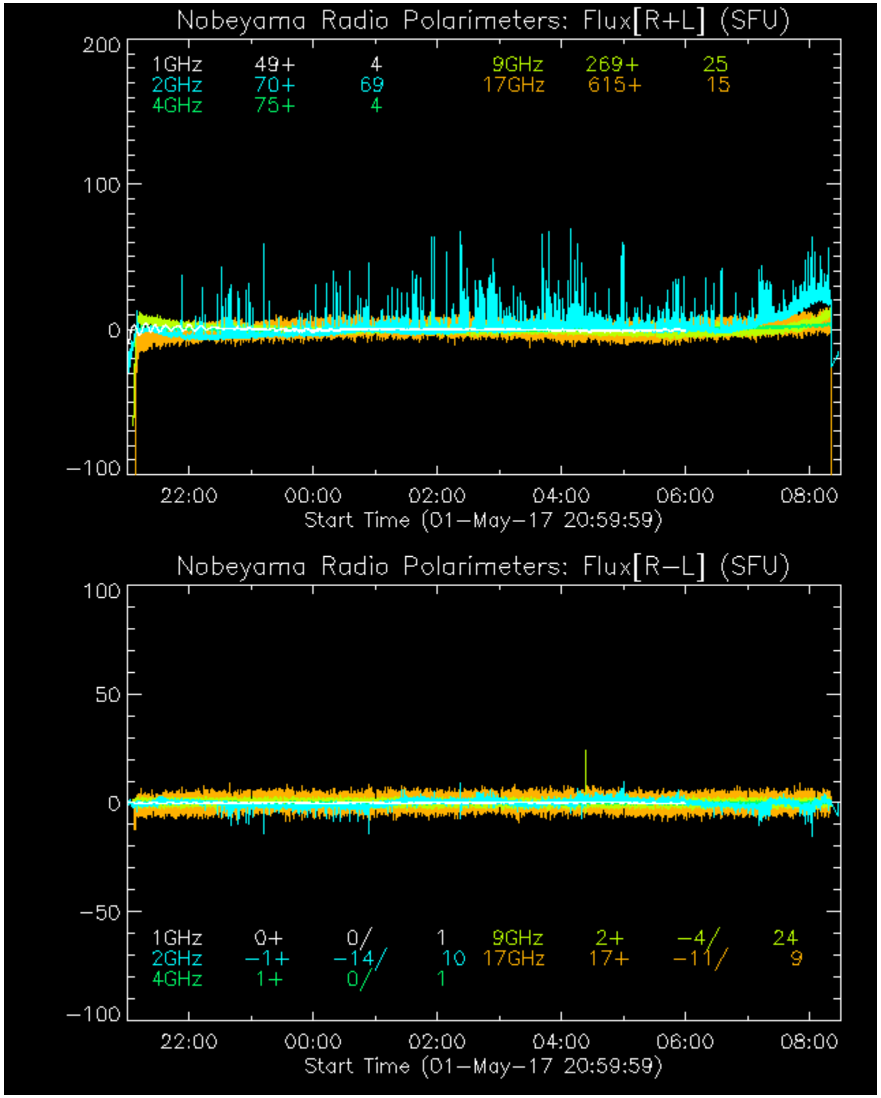

Result: Two light curves
Pros: Good time resolution, polarisation
Cons: No spatial, spectral information

Methods of radio astronomy

Radio polarimetry

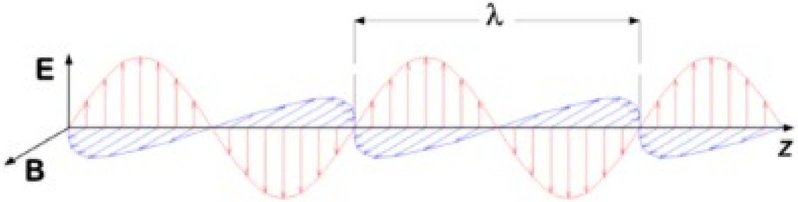

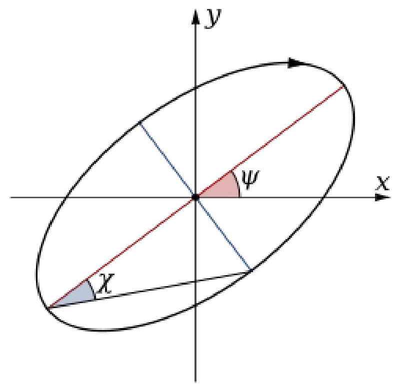

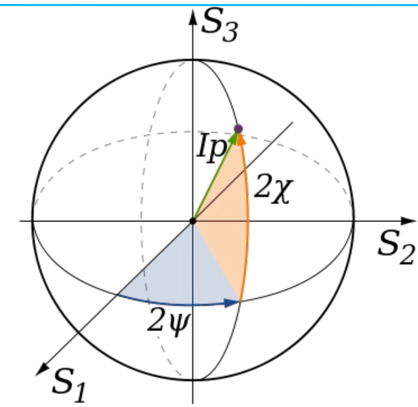

Polarisation: Stokes vector

$$\vec{S} = \begin{pmatrix} S_0 \\ S_1 \\ S_2 \\ S_3 \end{pmatrix} = \begin{pmatrix} I \\ Q \\ U \\ V \end{pmatrix}$$

$$S_0 = I$$
$$S_1 = Ip\cos 2\psi \cos 2\chi$$
$$S_2 = Ip\sin 2\psi \cos 2\chi$$
$$S_3 = Ip\sin 2\chi$$

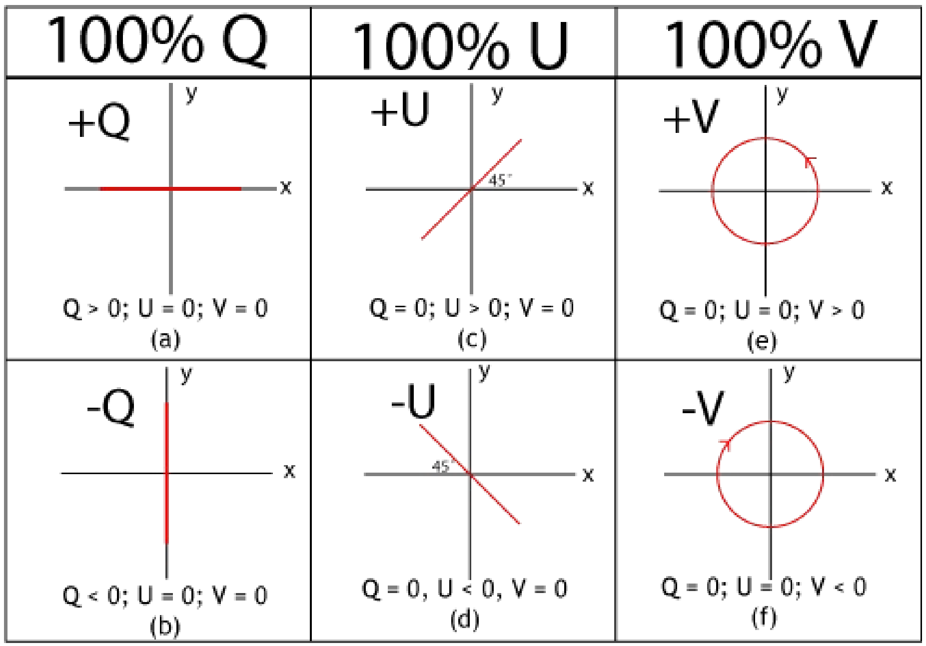

Radio polarimetry

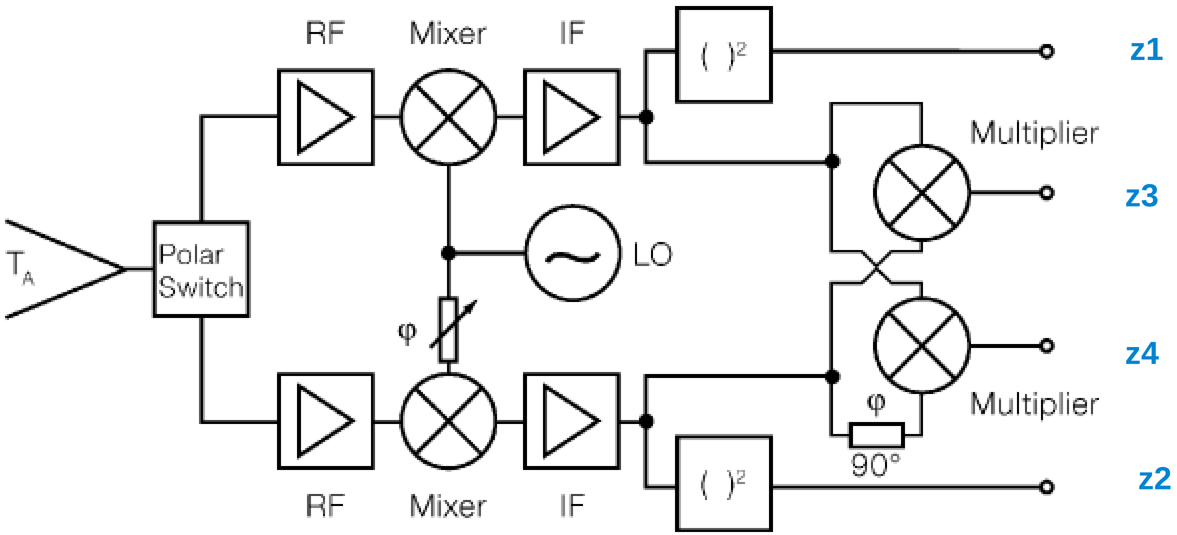

- output z_1 is IF 1 detected by a square-law detector,
- output z_2 is IF 2 detected by a square-law detector,
- output z_3 is the correlation of IF 1 and IF 2,
- output z_4 is the correlation of IF 2 and IF 2 with a phase delay of $\pi/2$ in one of the channels.

$$\begin{aligned} I &= \mathrm{const}\,(z_1 + z_2)\,, \\ Q &= \mathrm{const}\,(z_1 - z_2)\,, \\ U &= 2\,\mathrm{const}\,z_3\,, \\ V &= 2\,\mathrm{const}\,z_4\,. \end{aligned}$$

Methods of radio astronomy

Single-dish imaging

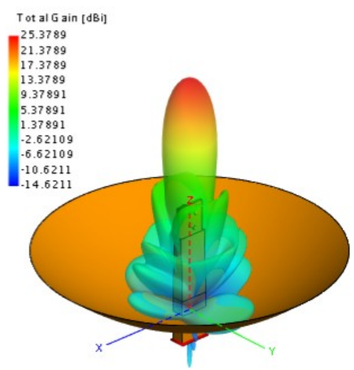

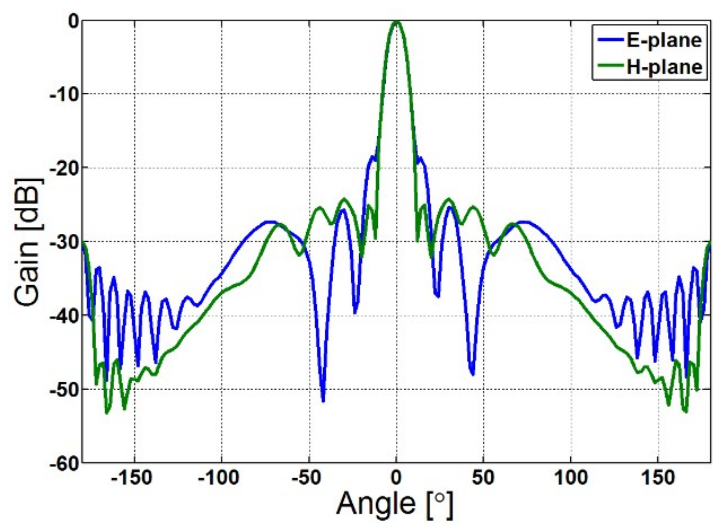

Result: Radio map with moderate spatial resolution
Pros: Degraded but real image
Cons: No spectral information, limited spatial resolution, worse time resolution

Methods of radio astronomy

Single-dish imaging

ALMA Fast TP scanning

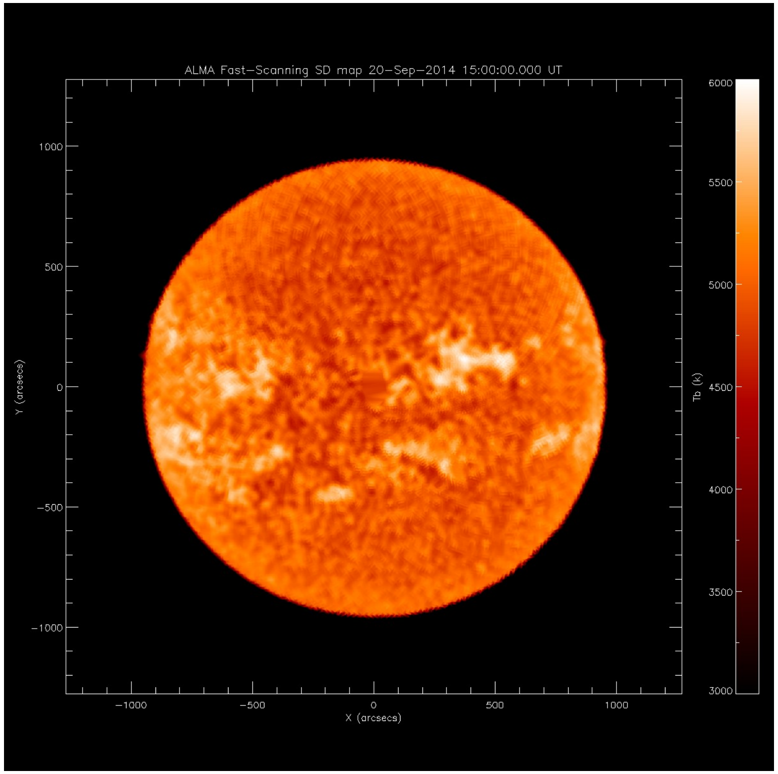

ALMA single-dish image of the Sun

Methods of radio astronomy

Single-dish imaging

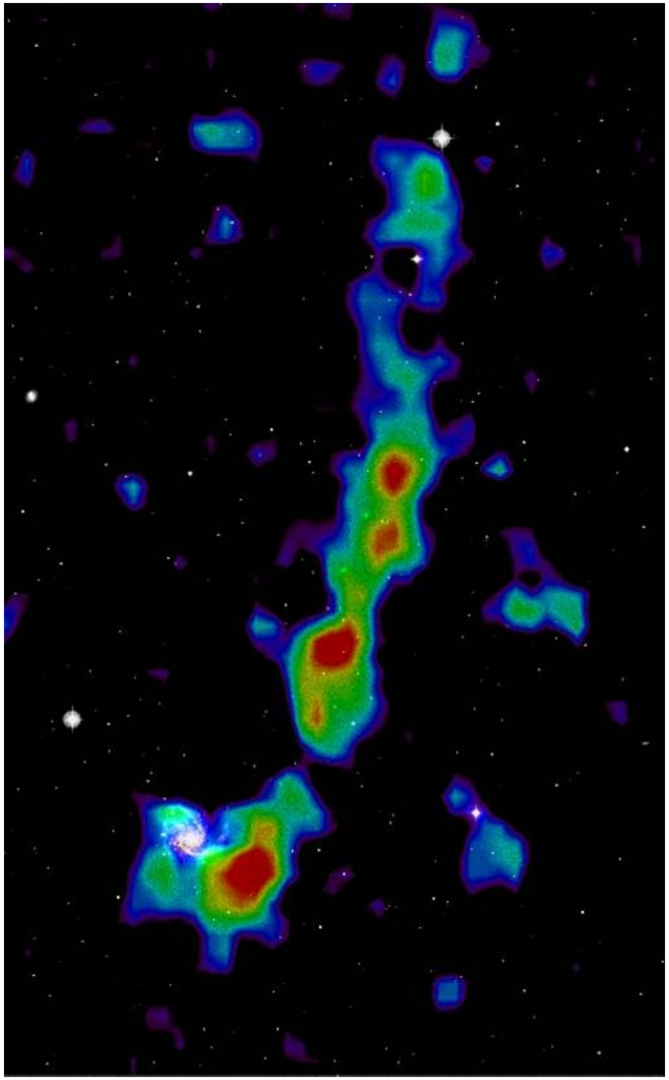

Gas tail behind a galaxy

Methods of radio astronomy

Single-dish imaging

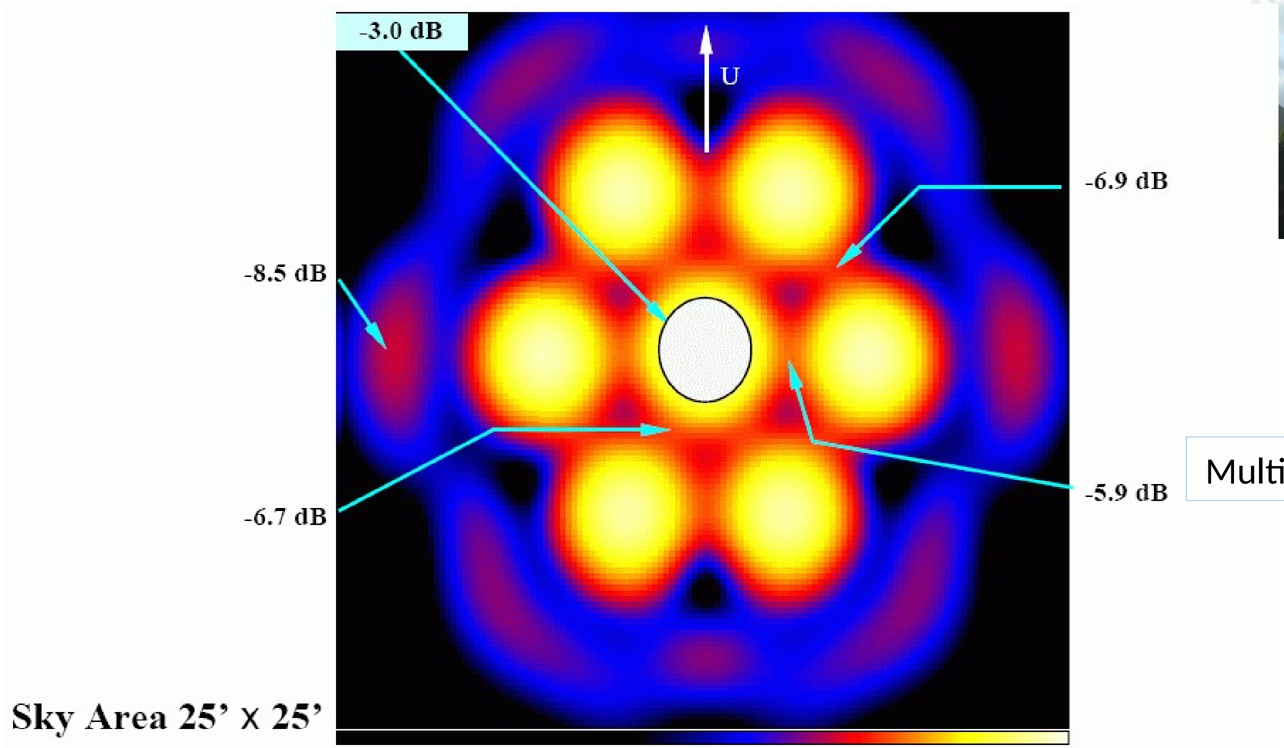

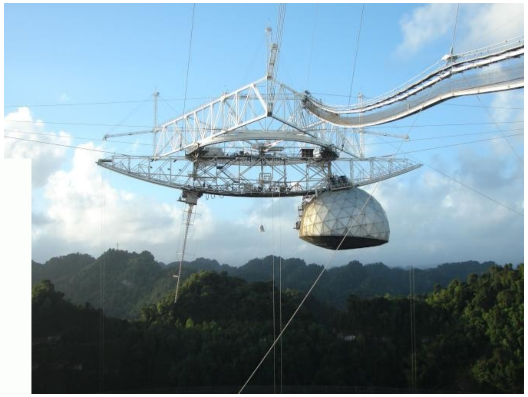

Multi-beam systems: ALFA @ Arecibo

Trends: Multi-feed arrays – „CCDs“ for radio astronomy

Sigle-feed:

FoV given by a **primary beam** of a single antenna (ALMA 12m: ~ 1'@100GHz). For larger fields we use mosaicing (i.e. consecutive re-pointing).

Multi-feed:

Larger FoV, faster mosaicing/scanning

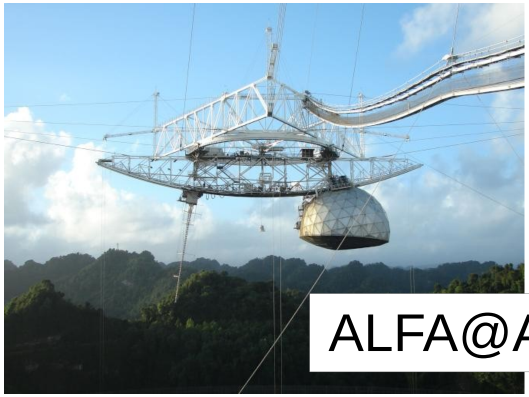

ALFA@Arecibo

Phased multi-array@ASKAP

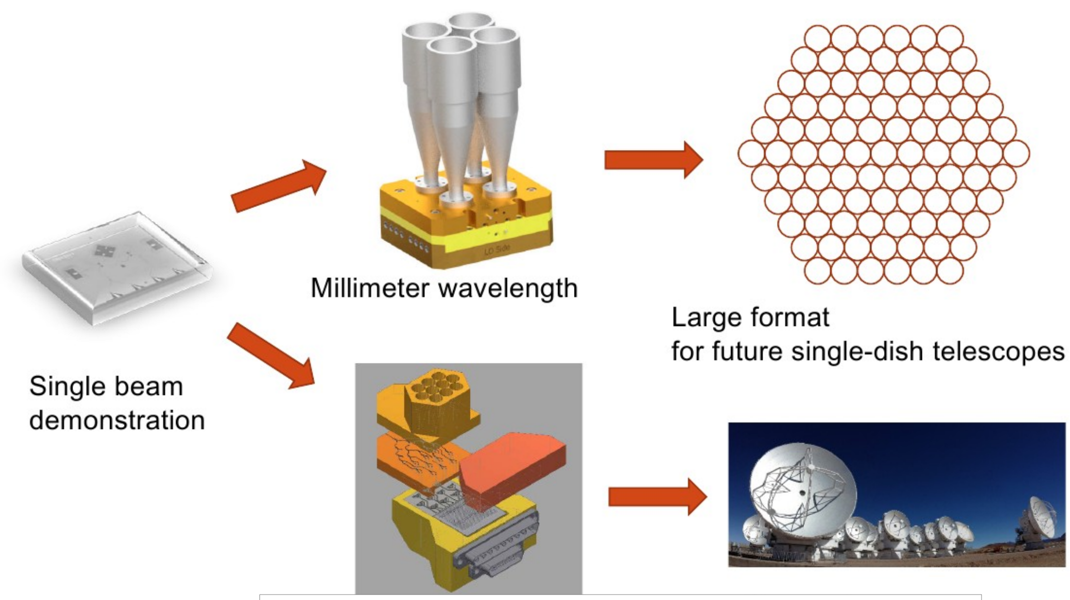

Applications nowadays even in mm/sub-mm range

(see ALMA Development Workshop 2019 on-line proceedings)

Methods of radio astronomy

Active radio astronomy: Radar sounding

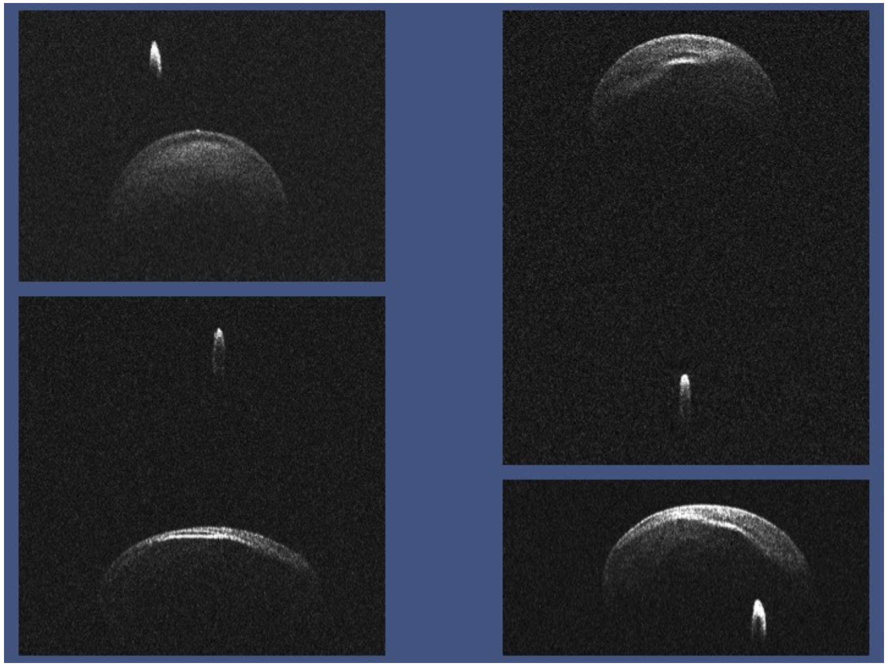

Binary asteriod KW4 by Arecibo

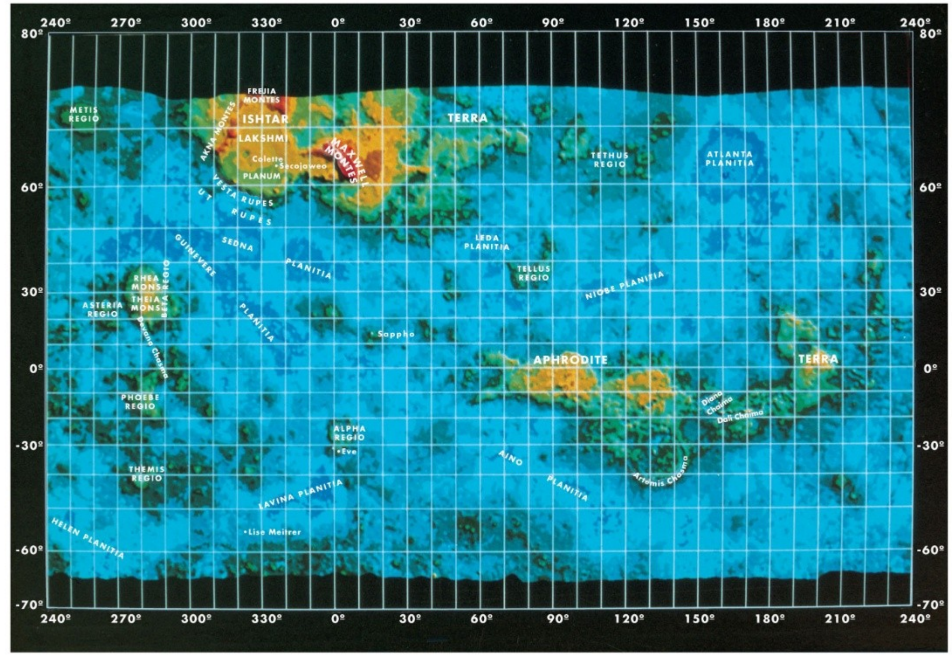

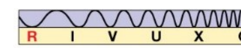

Venus surface (Magellan)

Active radio astronomy: Radar sounding

Radar Equation

We begin by reviewing the basic monostatic radar range equation describing received power for a radar system:

$$P_r = \frac{P_t G_t G_r \lambda^2 PF^4 \sigma_{RCS}}{(4\pi)^3 r^4 L}$$

Where P_t = Transmitted power
G_t = Transmit antenna gain
G_r = Receive antenna gain
λ = Radar wavelength
PF = Pattern Propagation Factor
r = Slant range from radar to target
σ_{RCS} = Target radar cross section (RCS)
L = Miscellaneous system losses

$$R_{\max} = \sqrt[4]{\frac{P_S \cdot G^2 \cdot \lambda^2 \cdot \sigma}{P_{E_{\min}} \cdot (4\pi)^3 \cdot L_{ges}}}$$

Methods of radio astronomy

Active radio astronomy: Radar sounding

Arecibo – had an active radar

FAST:
just a passive radio telescope

Methods of radio astronomy

Active radio astronomy: Radar sounding

Radar-based meteor research

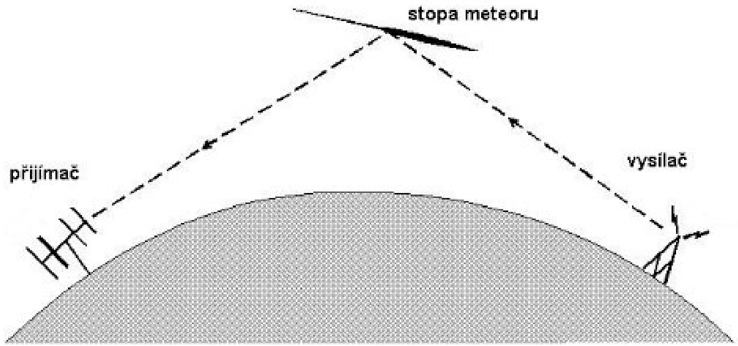

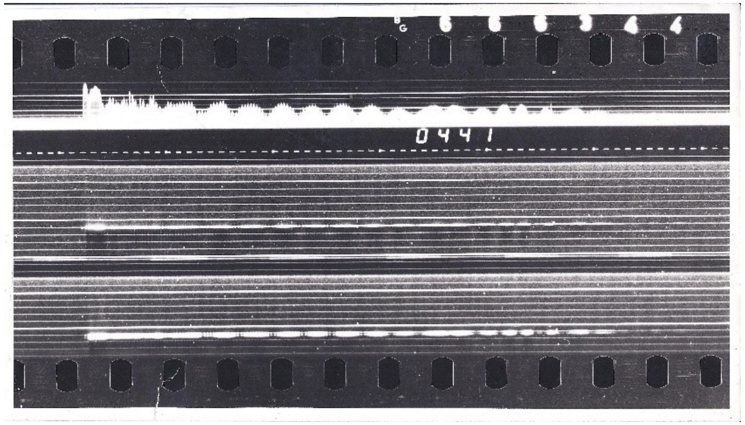

Amateur radio observations of meteors
e.g. http://bolidozor.cz

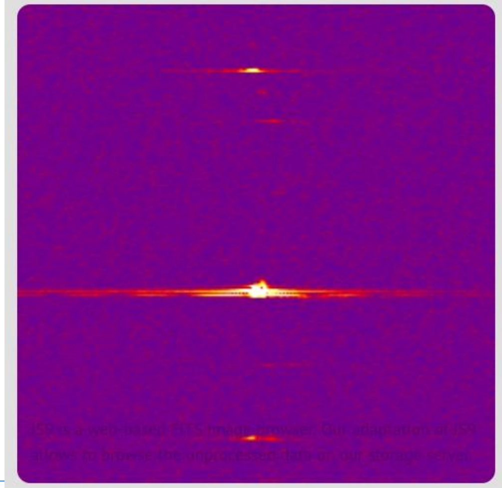

Methods of radio astronomy

Active radio astronomy: Radar sounding

EISCAT3D: Ionospheric sounding + space debris search

Phased-array radar

Phased radar GIF

Methods of radio astronomy

(single-dish) Radio spectroscopy

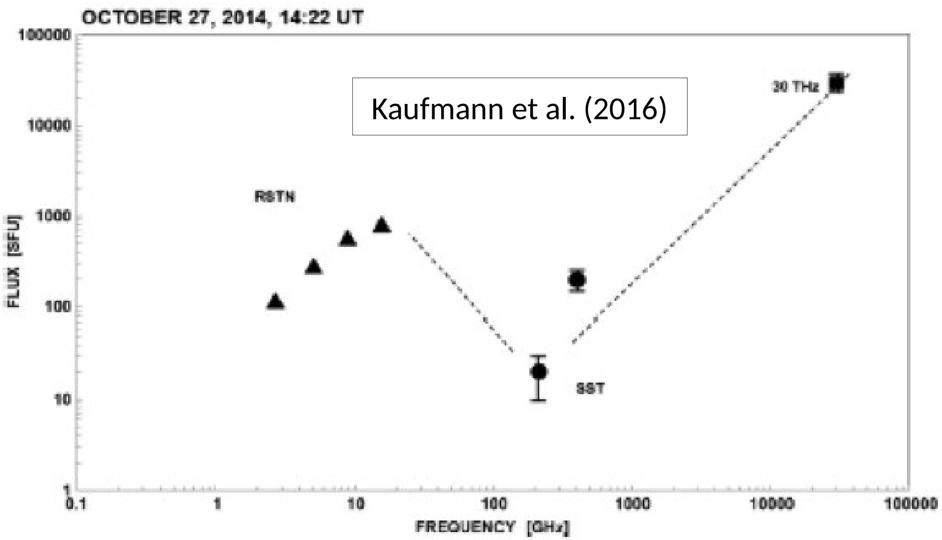

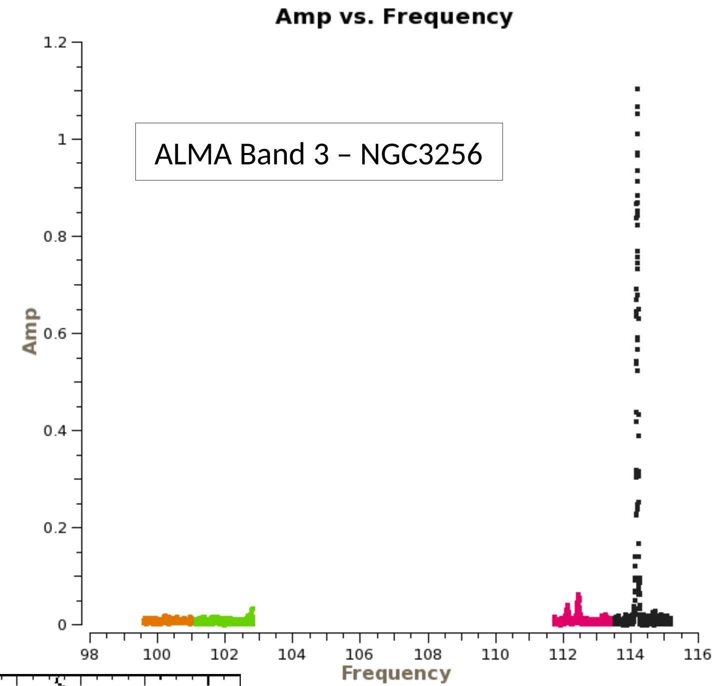

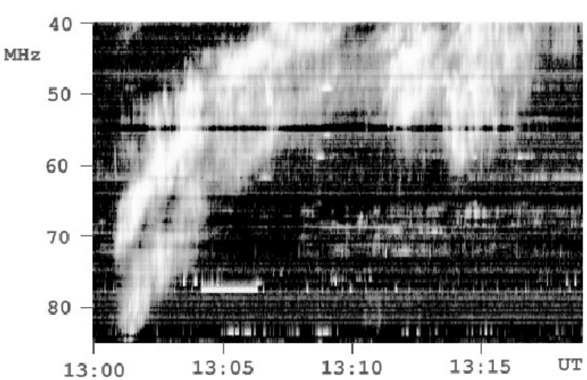

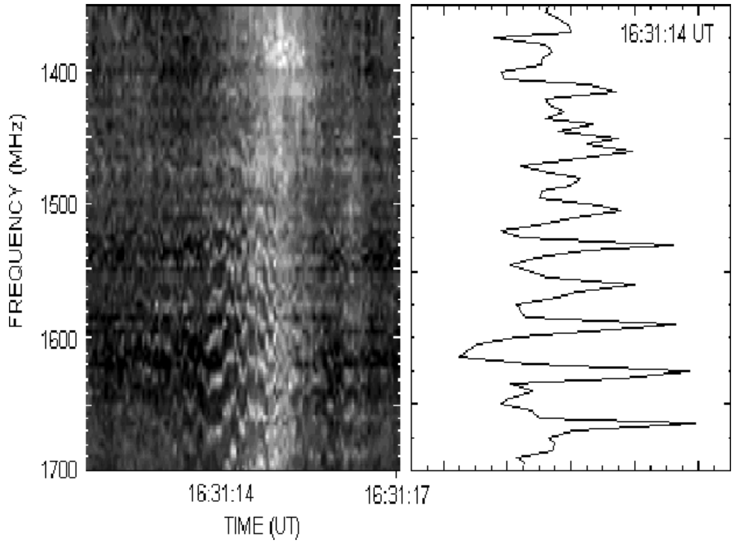

Result: (dynamic) spektra

Pros: (rather) Good time resolution full spectra

Cons: No spatial resolution

Methods of radio astronomy

(single-dish) Radio spectroscopy

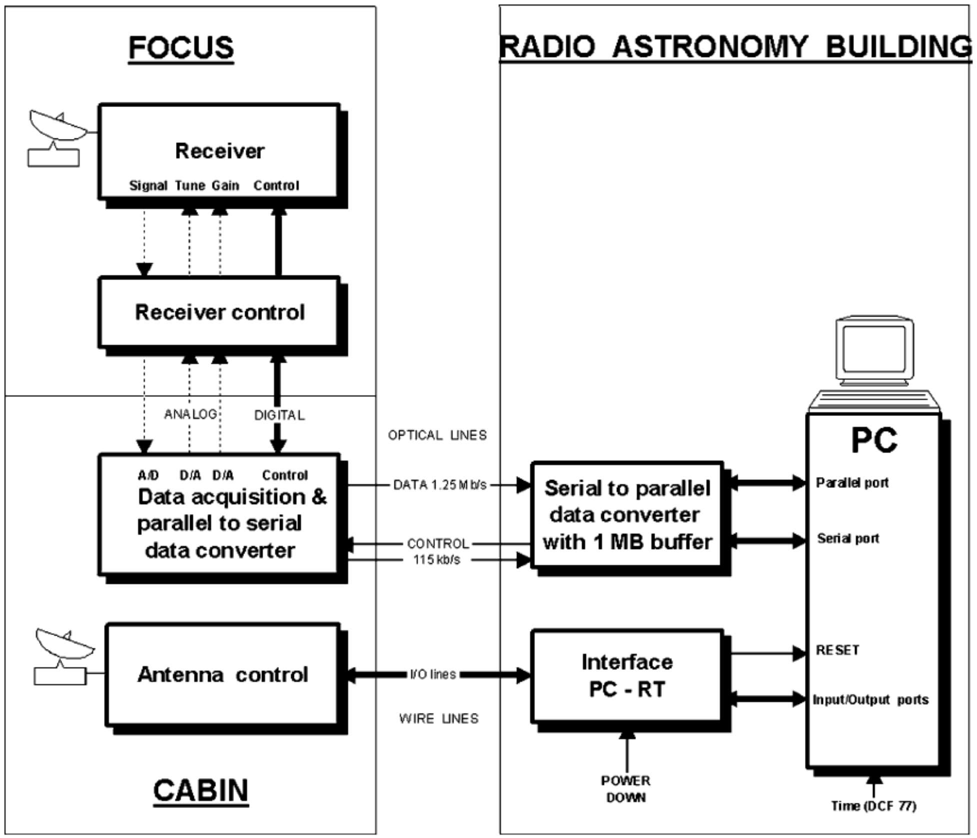

RT5 @ Ondrejov: Sweeping spectrograph

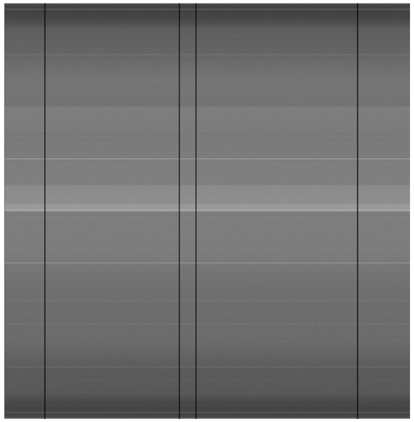

Δf = 250 kHz
Δt =1 ms

RT5 @ Ondrejov: New tested Fourier-based (autocorr) spectrograph - 1st results

Methods of radio astronomy

(single-dish) Radio spectroscopy/spectro-polarimetry

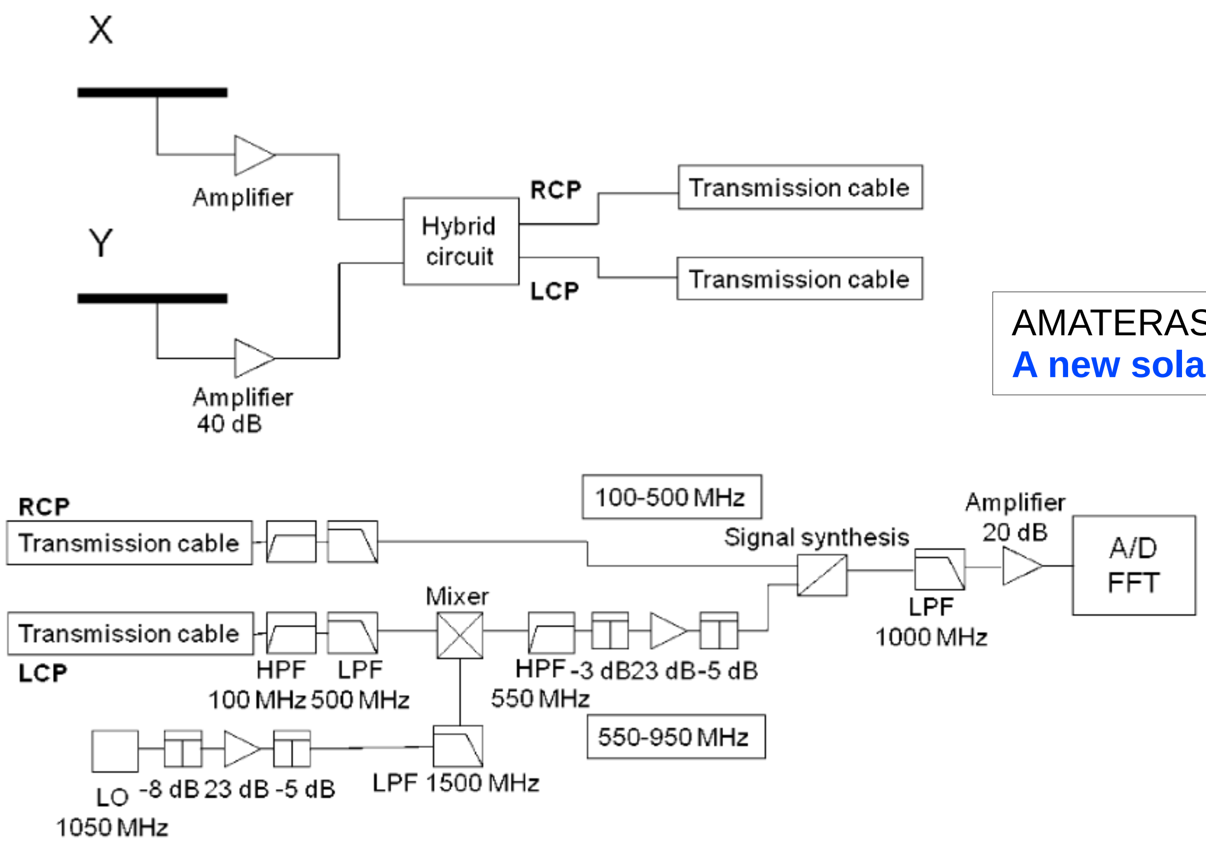

Figure 2 Block diagram of IPRT/AMATERAS.

AMATERAS/IPRT Nobeyama, Japan
A new solar radio spectorgraph @ Ondrejov

DSP technology now affordable for small & middle-size observatories

Spectrographs/spectro-polarimeters built as Software-Defined Radio
Ondrejov Solar hi-Cadence Automated Radio Spectrograph(s) / OSCARS

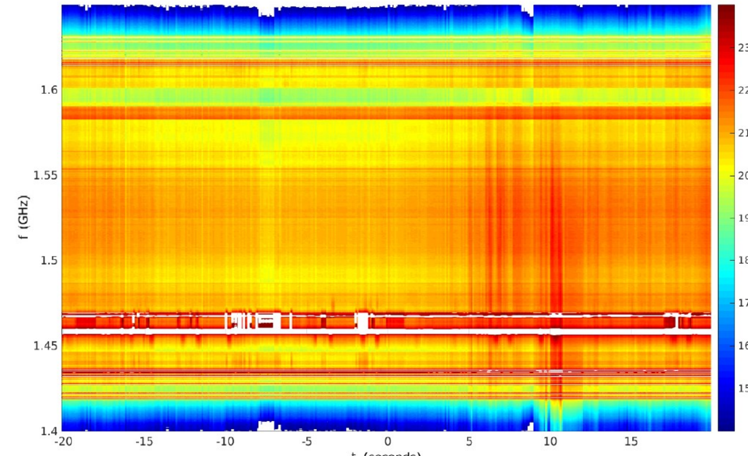

(Puričer, Kovář & Bárta, Electronics 2019)

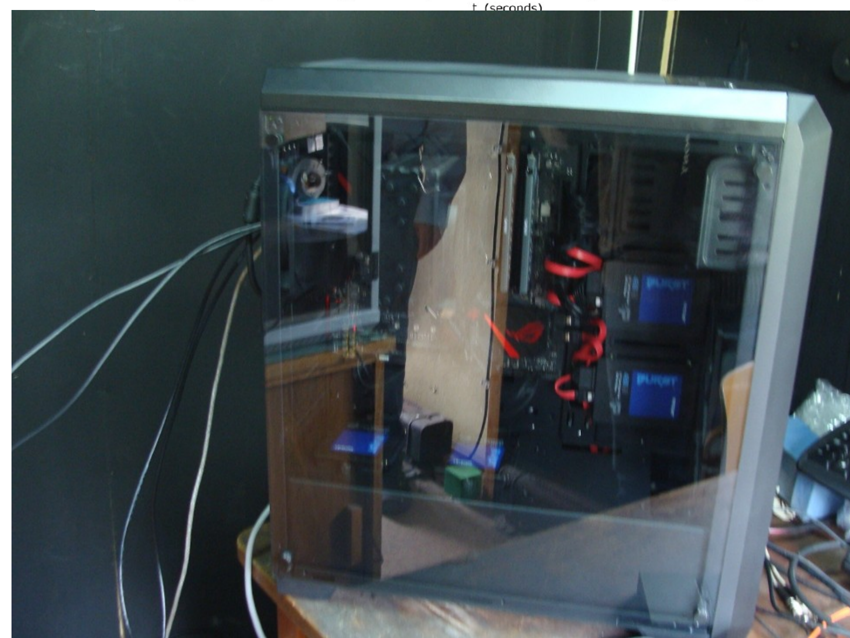

Methods of radio astronomy

Radio spectro-polarimetry

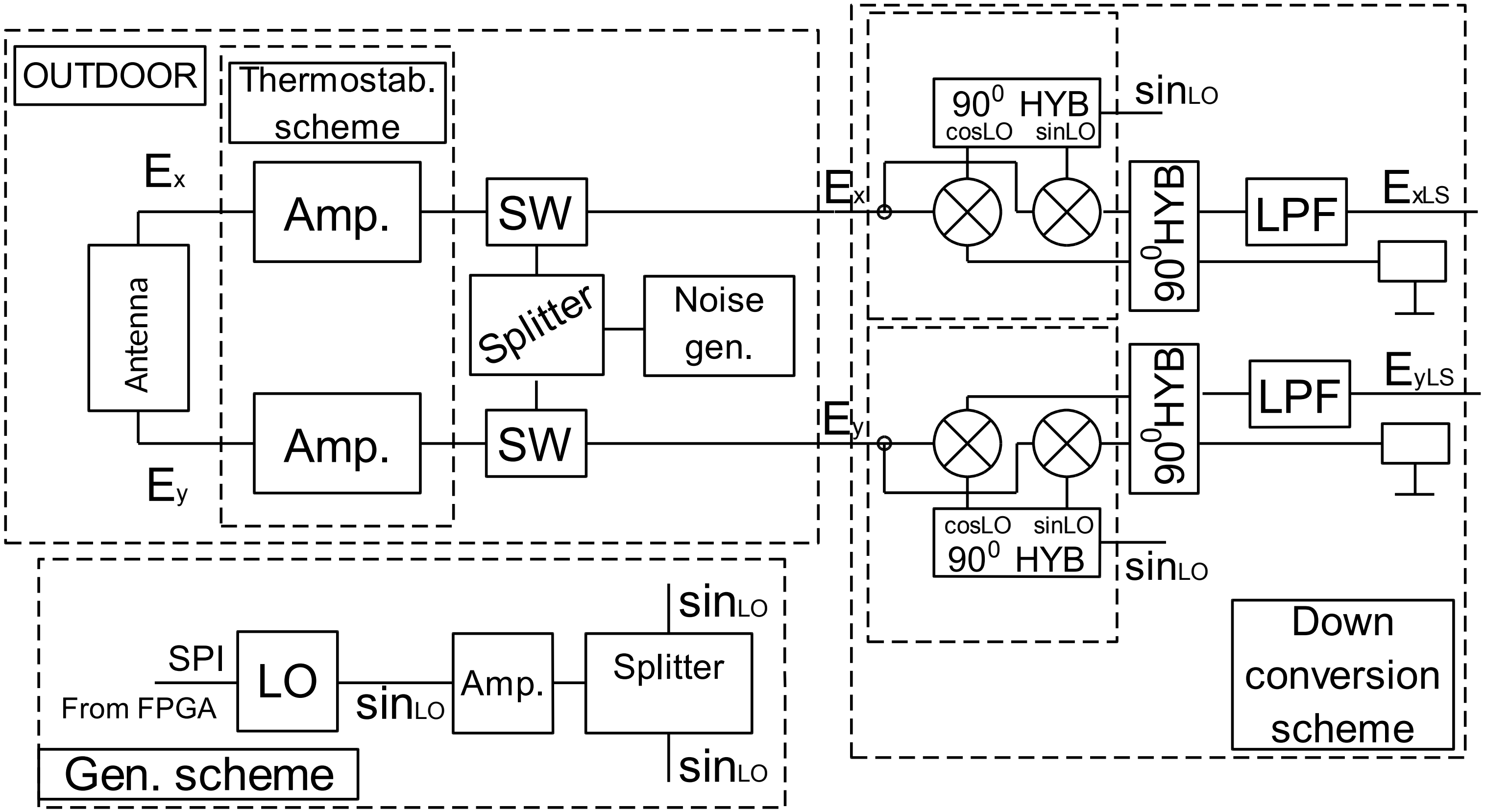

SSPM Badary/Irkutsk, Russia

Methods of radio astronomy

Radio spectro-polarimetry

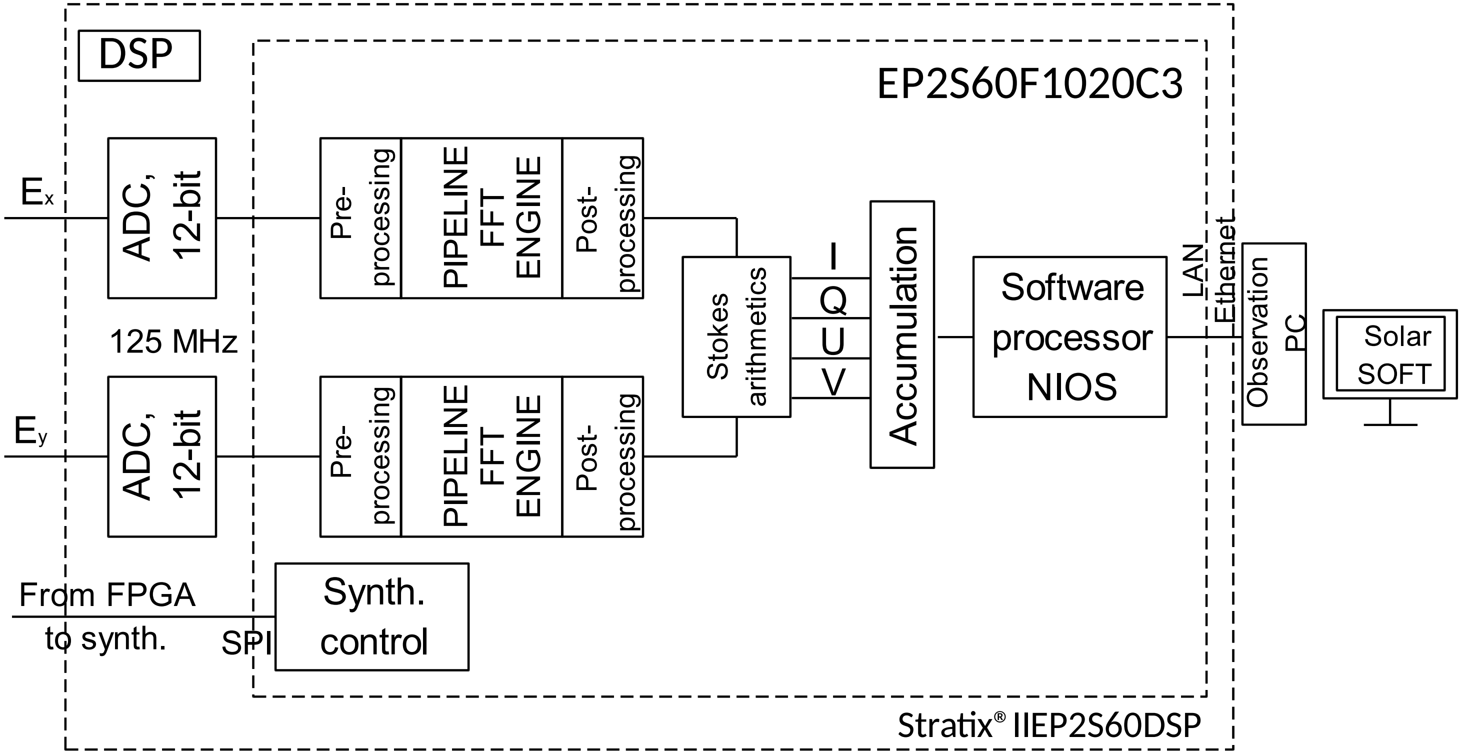

SSPM Badary/Irkutsk, Russia

Methods of radio astronomy

Radiospectro-polarimetry

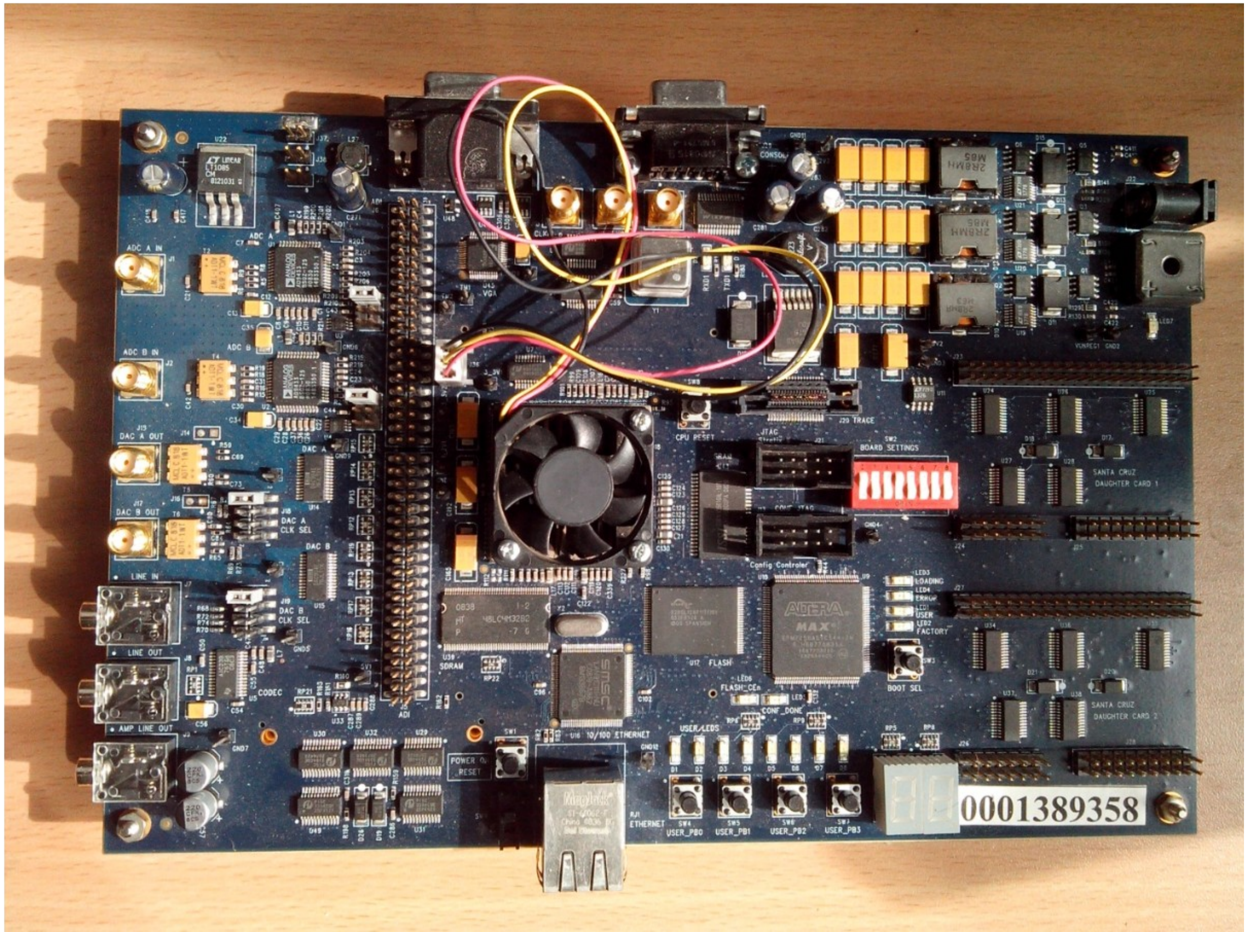

SSPM Badary/Irkutsk, Russia

Methods of radio astronomy

Radiospectro-polarimetry

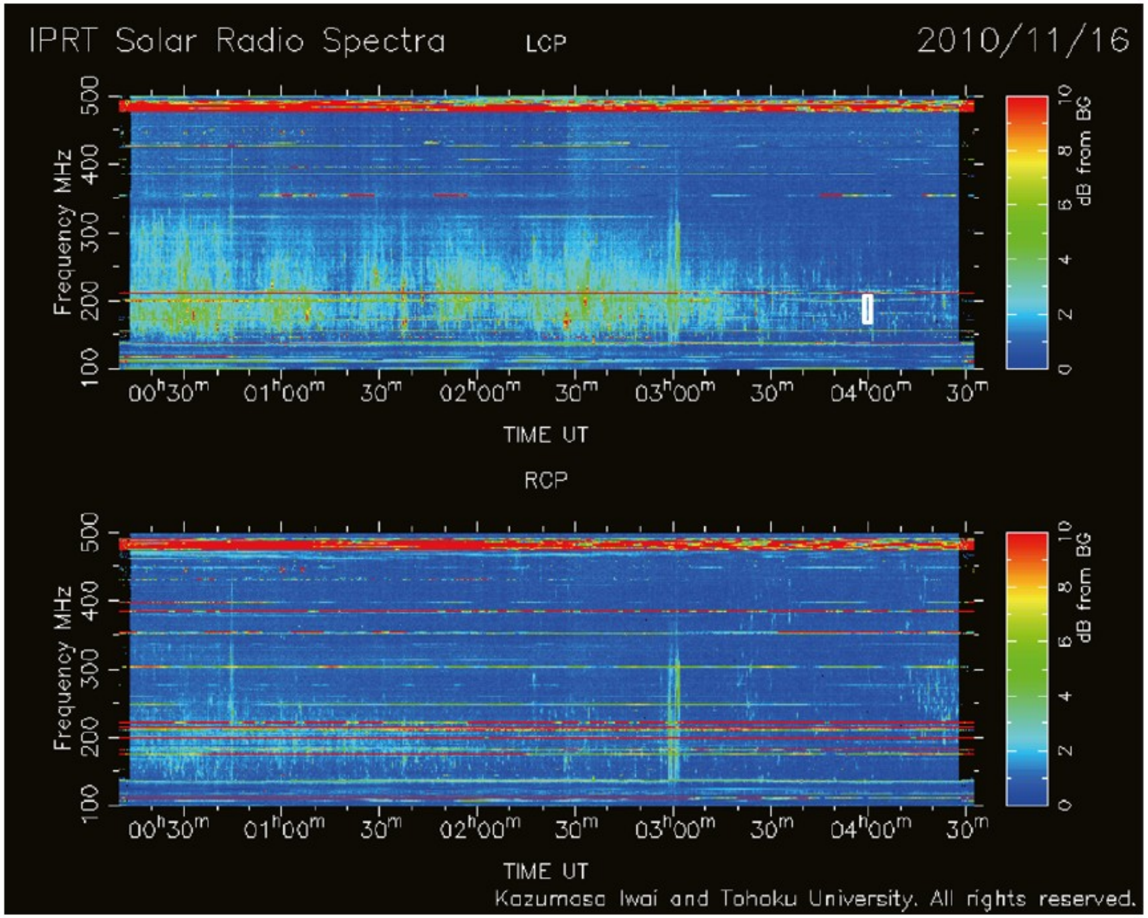

Result: (dynamic) spektra

Pros: (rather) Good time resolution, full spectra, **polarisation**

Cons: No spatial resolution

Radio interferometry

Phased arrays – sparse rows

$$|I_\Sigma(\theta)| = \frac{1 - \cos \mathrm{N}\frac{2\pi D}{\lambda}\theta}{1 - \cos\frac{2\pi D}{\lambda}\theta}$$

Aperture synthesis – baseline signal correlations

$$\langle I_{AB}\rangle(\theta) = \int_{-\infty}^{+\infty} B(\theta)\exp\left(i\frac{2\pi D}{\lambda}\theta\right)d\theta$$

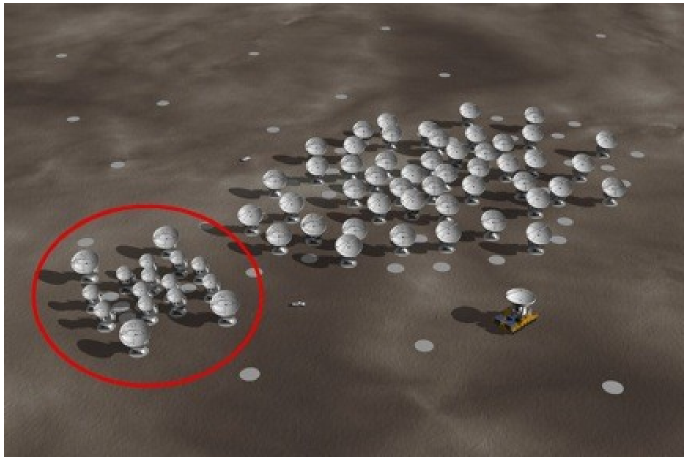

Radio spectroscopy in closer view

Methods of radio astronomy

Solar radio dynamic spectroscopy

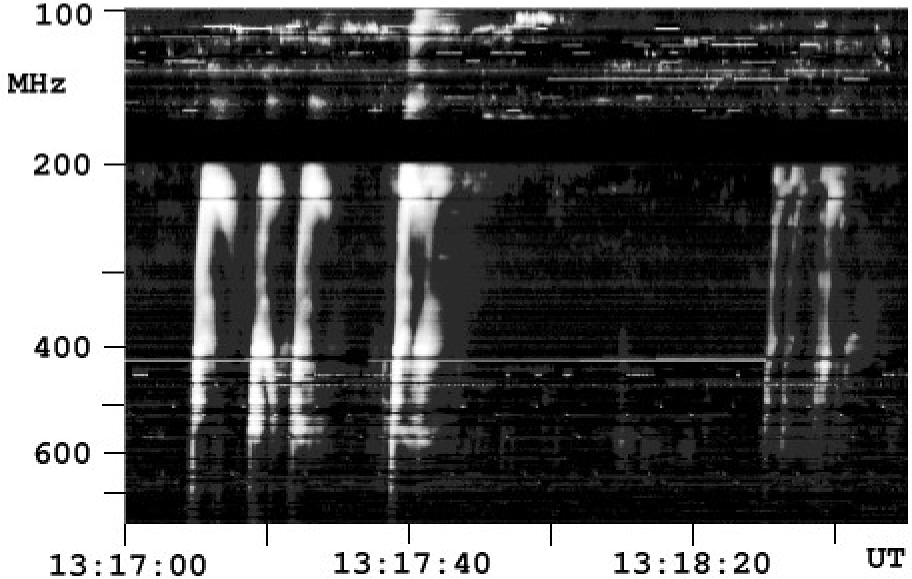

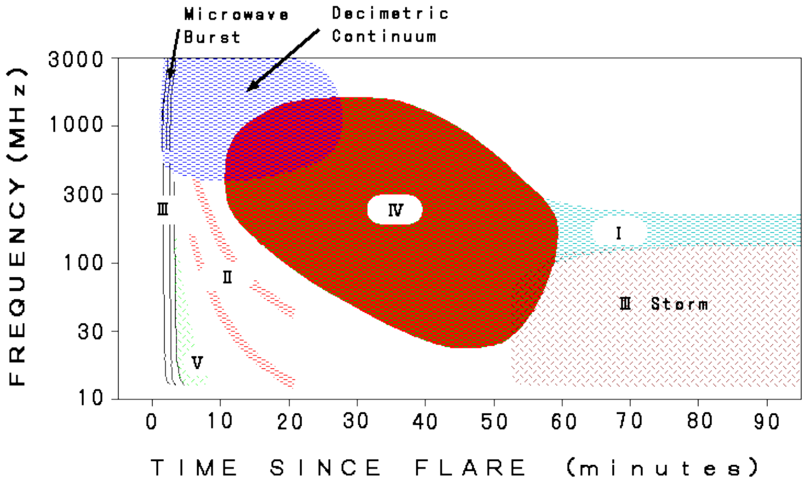

$$\omega_{\mathrm{pe}} = \sqrt{\frac{n_e e^2}{m^* \varepsilon_0}}$$

$$f_{\mathrm{pe}} \approx 8980\sqrt{n_e}\ \mathrm{Hz}$$

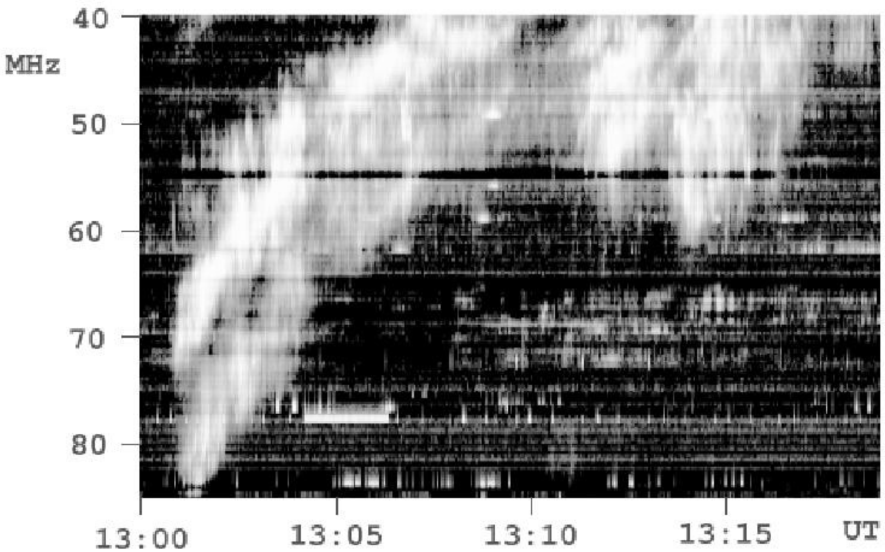

Methods of radio astronomy

Solar radio dynamic spectroscopy

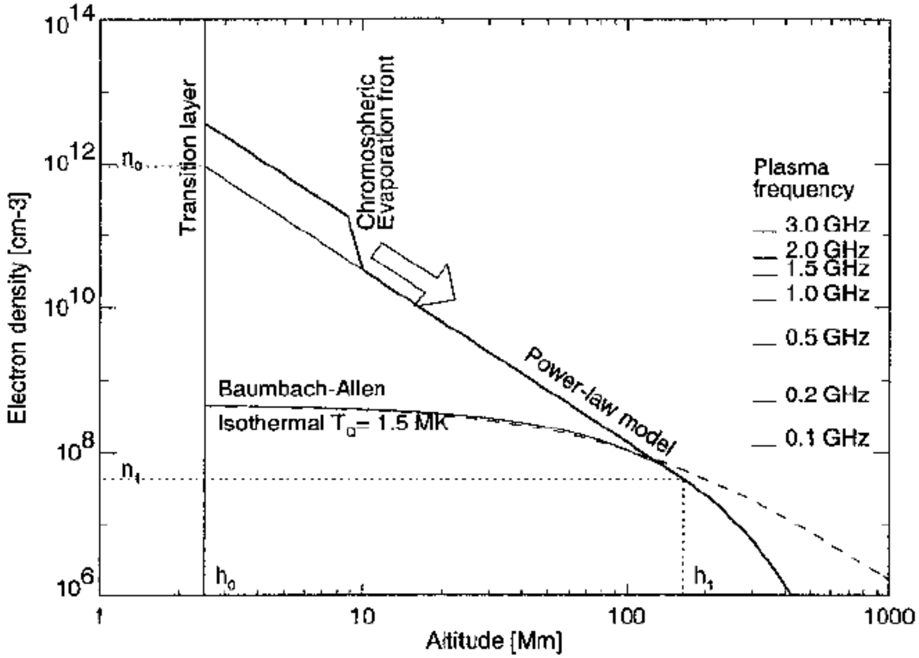

$$\omega_{\mathrm{pe}} = \sqrt{\frac{n_{\mathrm{e}} e^2}{m^* \varepsilon_0}}$$

$$f_{\mathrm{pe}} \approx 8980 \sqrt{n_{\mathrm{e}}} \text{ Hz}$$

$$\frac{\Delta f}{\Delta t} = \frac{\Delta f}{\Delta n} \cdot \frac{\Delta n}{\Delta h} \cdot v$$

$$n(h) = n_1 \left(\frac{h}{h_1} \right)^{-p}$$

$$v = 4.55 \times 10^{14} f^{-1.84} \frac{\mathrm{d}f}{\mathrm{d}t}$$

Methods of radio astronomy

(Solar) radio dynamic spectroscopy

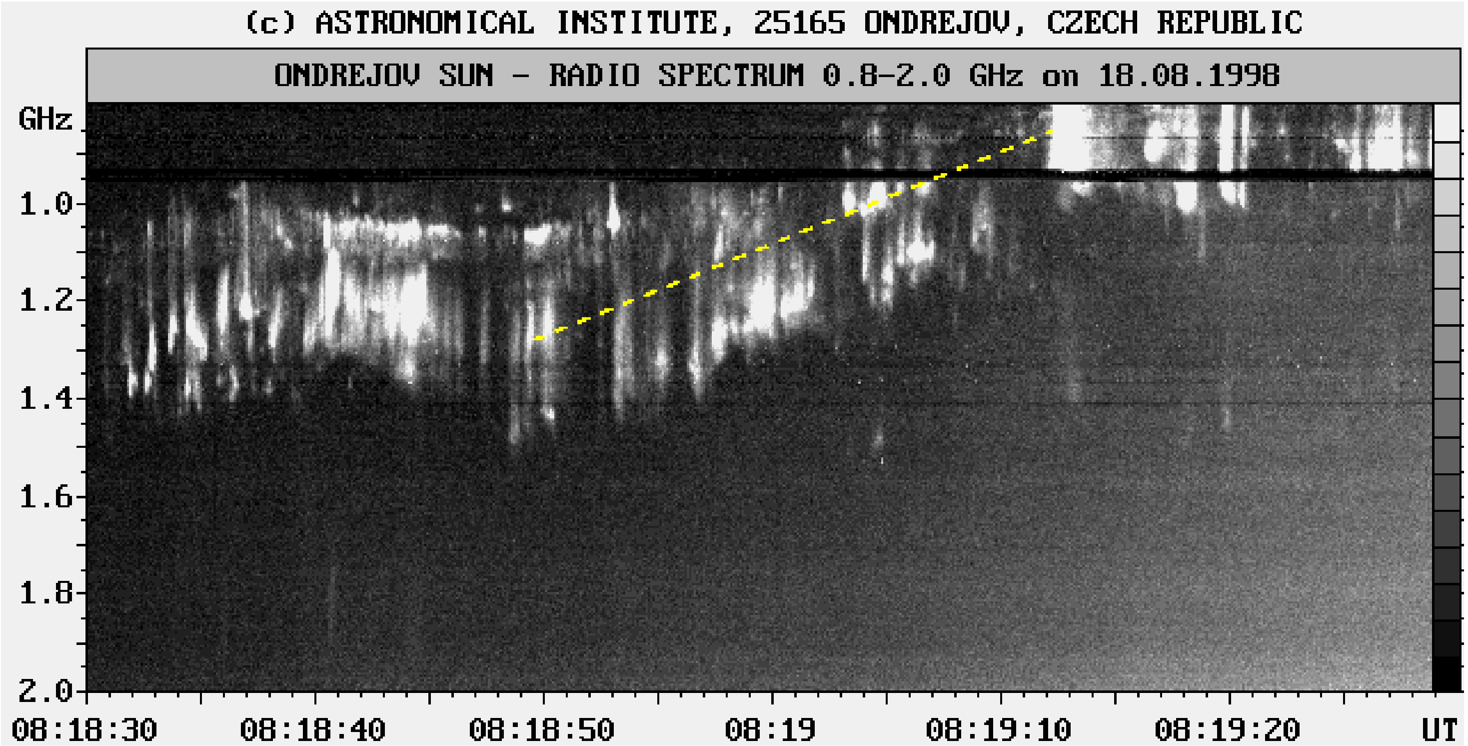

$$\frac{\mathrm{d}f}{\mathrm{d}t} = \frac{f_2 - f_1}{t_2 - t_1}$$

Frequency drift

Solar radio dynamic spectroscopy

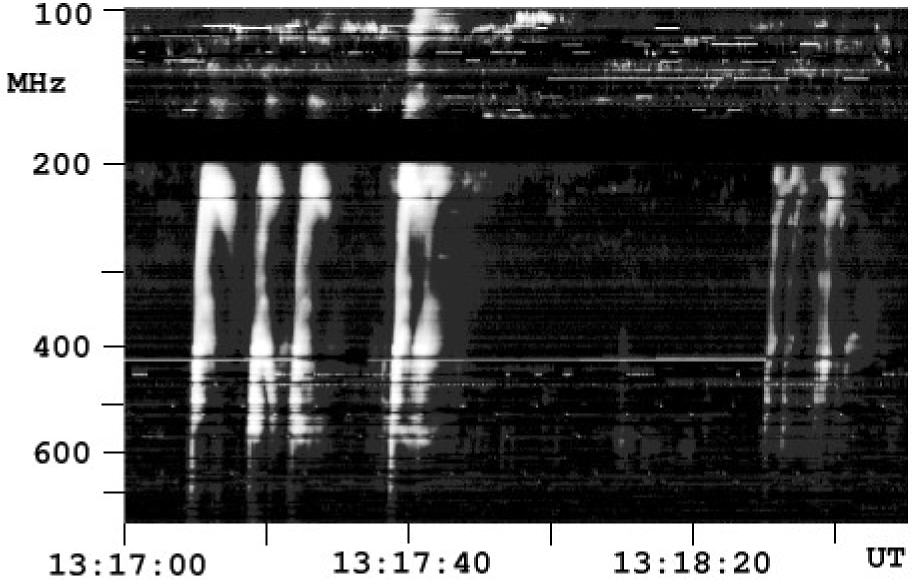

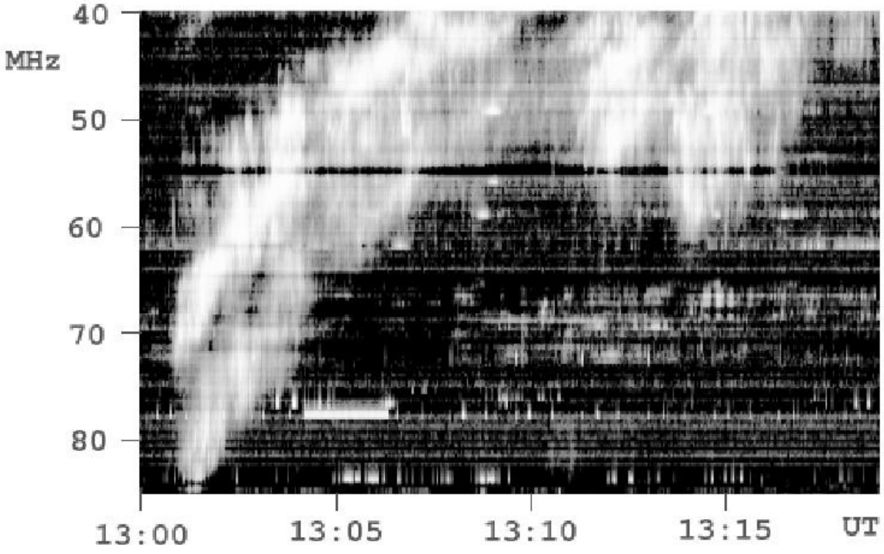

$$\omega_{\mathrm{pe}} = \sqrt{\frac{n_{\mathrm{e}} e^2}{m^* \varepsilon_0}}$$

$$f_{\mathrm{pe}} \approx 8980\sqrt{n_{\mathrm{e}}}\ \text{Hz}$$

$$\frac{\Delta f}{\Delta t} = \frac{\Delta f}{\Delta n} \cdot \frac{\Delta n}{\Delta h} \cdot v$$

$$n(h) = n_1 \left(\frac{h}{h_1}\right)^{-p}$$

$$v = 4.55 \times 10^{14} f^{-1.84} \frac{\mathrm{d}f}{\mathrm{d}t}$$

Plasmoid ejecta & DPS radio bursts

Karlicky 2004, Barta et al., 2008

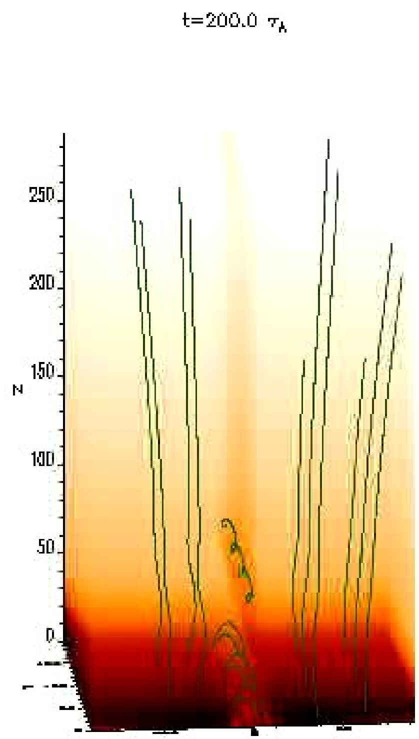

Bárta & Karlický, 2007

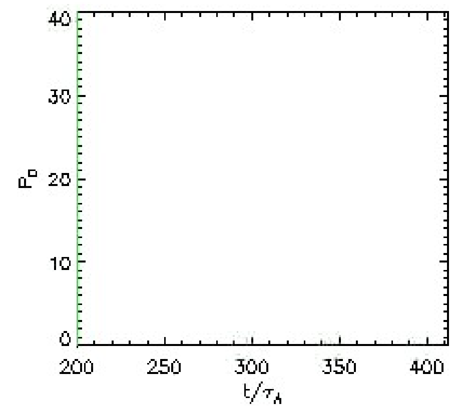

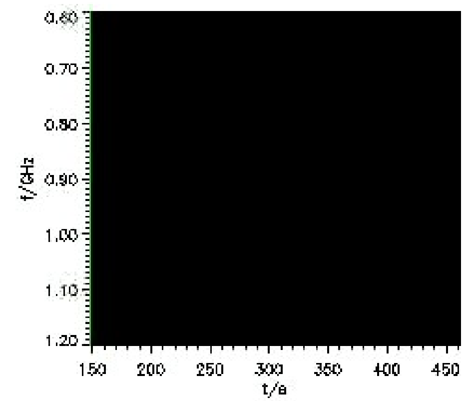

Model: DPS radio spectrum formation

Plasmoid ejecta & DPS radio bursts

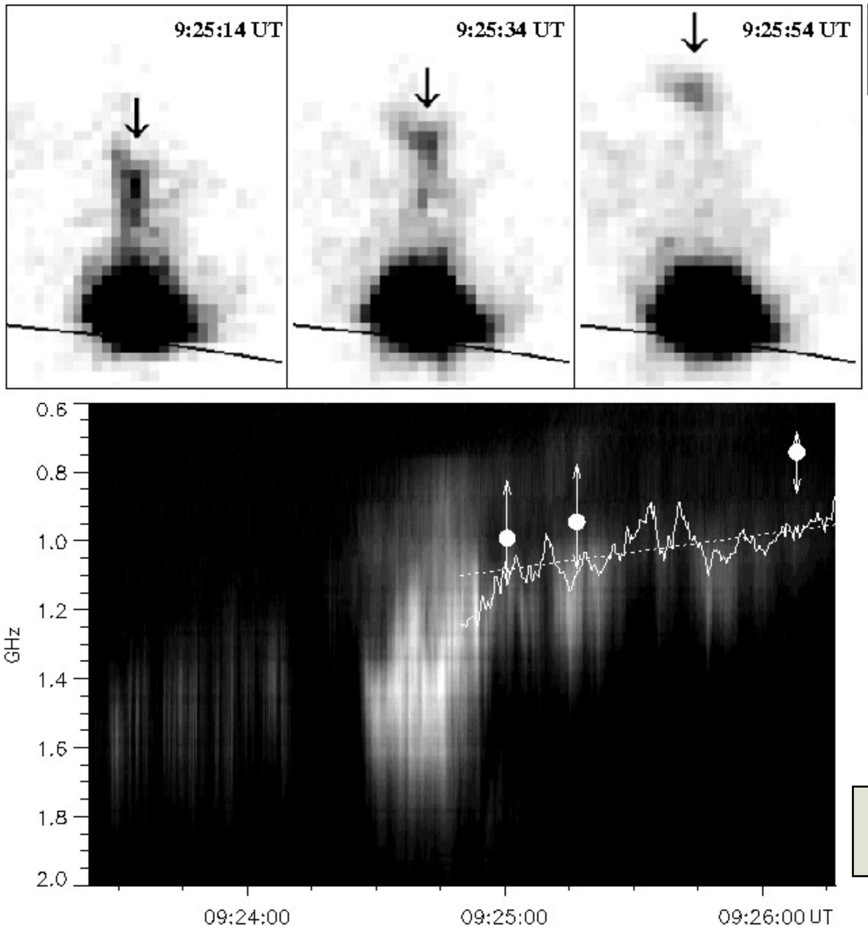

Ohyama & Shibata, 1998, ApJ 499

Kliem, Karlicky & Benz, 2000, A&A 360

Plasmoid ejecta & DPS radio bursts

Observation

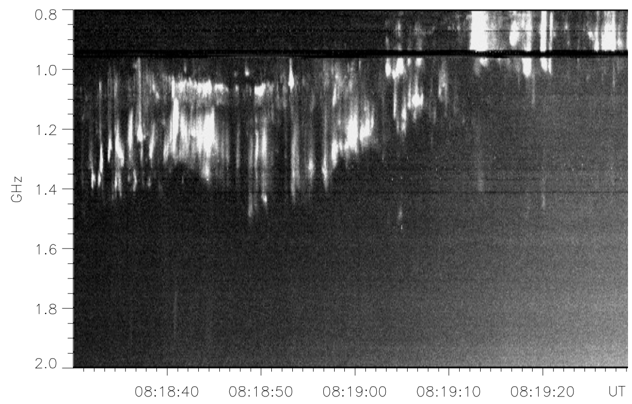

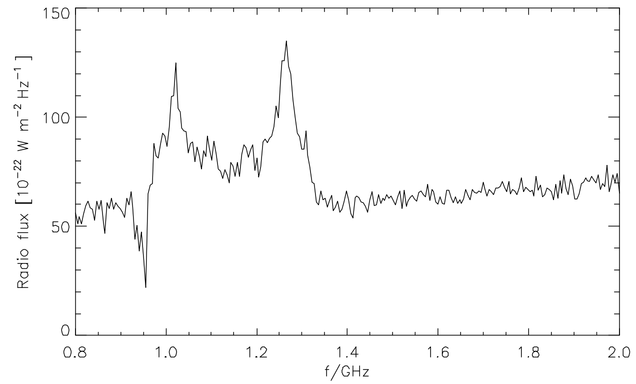

Model

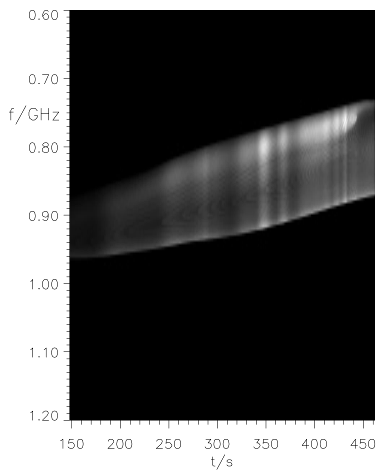

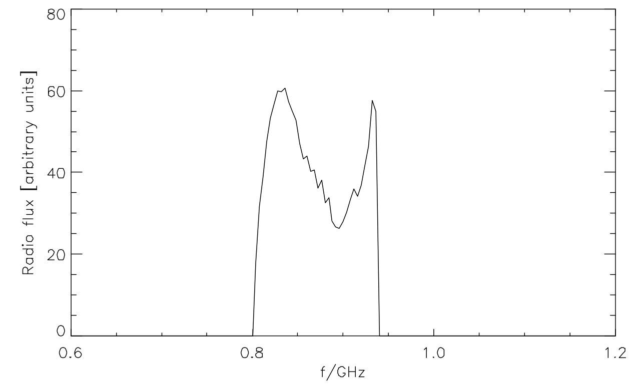

Barta, Karlicky & Zemlicka 2008, SPh

Relations to observation

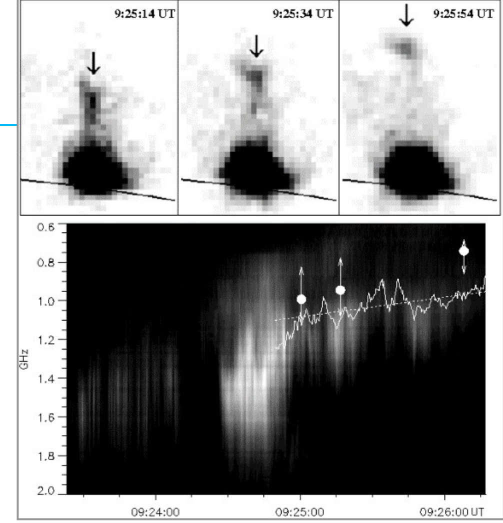

Plasmoid ejecta & DPS radio bursts

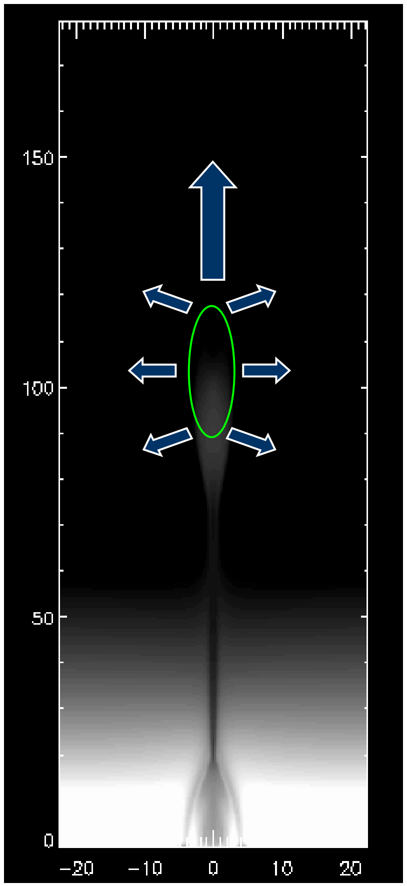

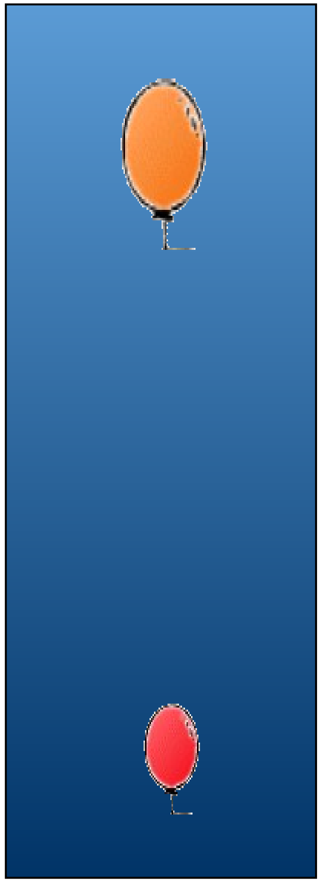

Model-based diagnostics

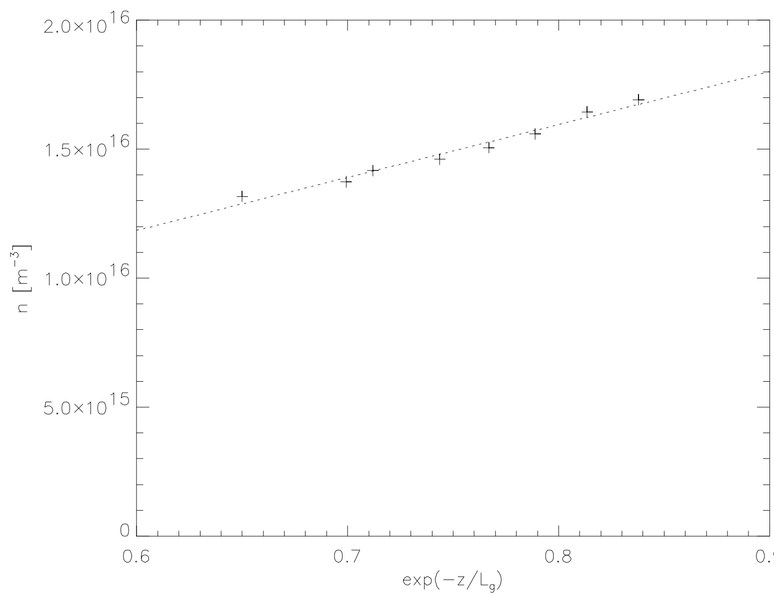

$$n_{\mathrm{in}} = \frac{p_0}{2k_{\mathrm{B}}T_{\mathrm{in}}} \cdot \exp\left(-\frac{z}{L_{\mathrm{g}}}\right) + \frac{B^2_{\mathrm{out}}}{4\mu_0 k_{\mathrm{B}} T_{\mathrm{in}}}$$

Radio signatures of turbulence in the reconnection outflows

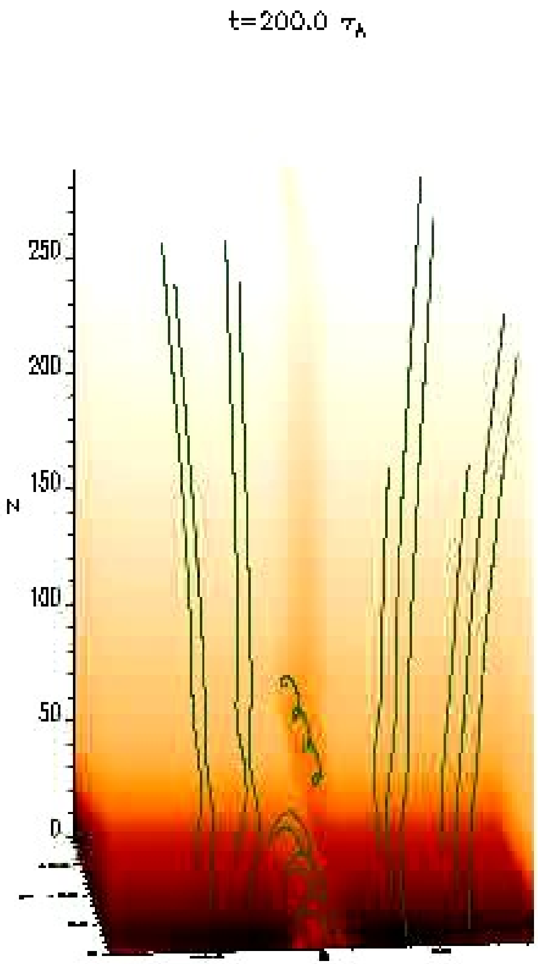

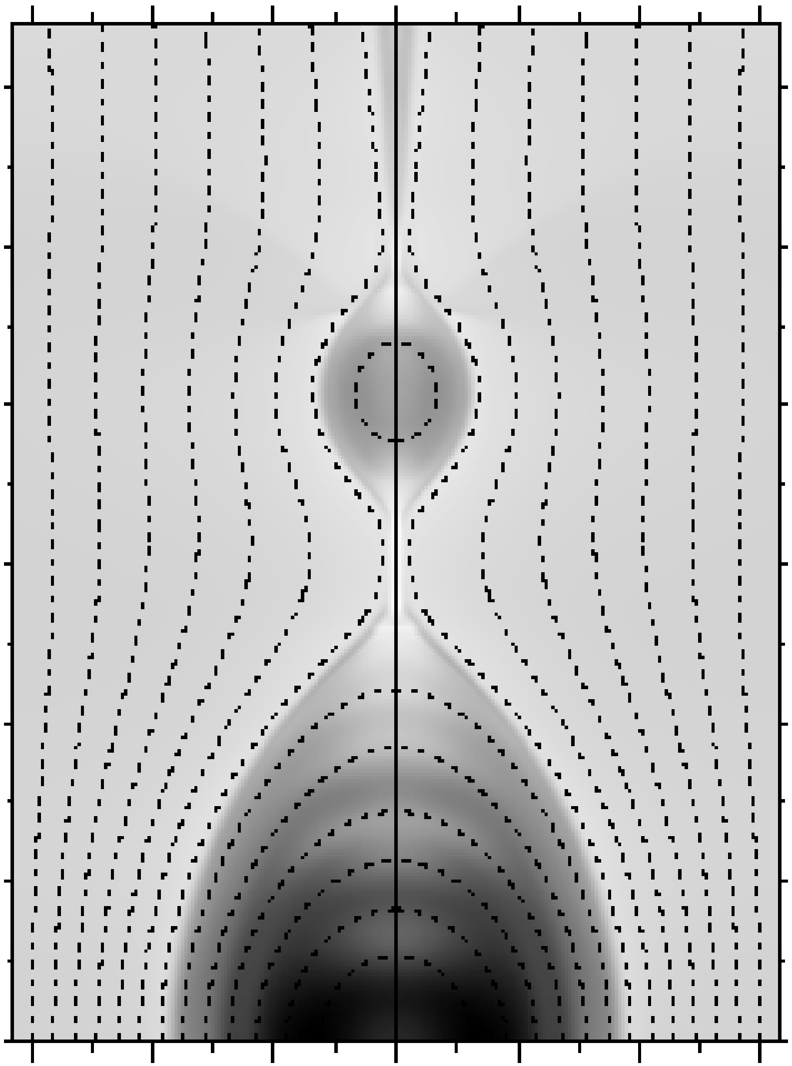

Methods of radio astronomy

Solar radio dynamic spectroscopy

Radio signatures of turbulence in the reconnection outflows

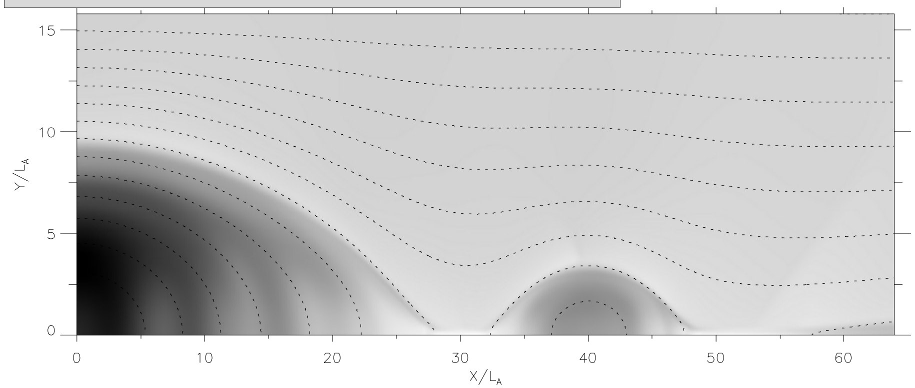

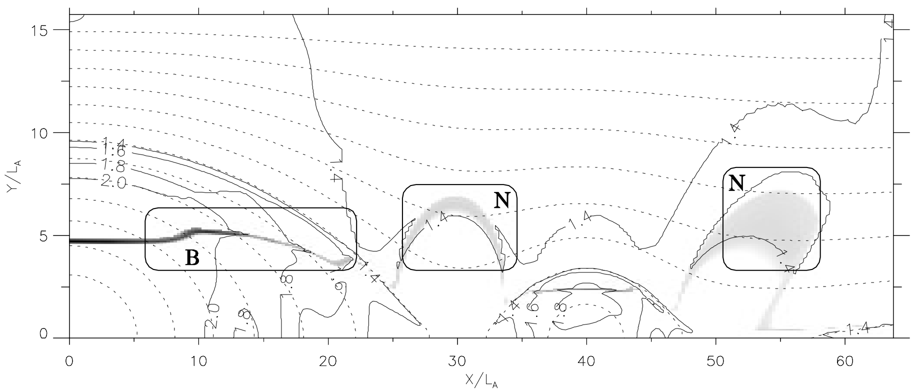

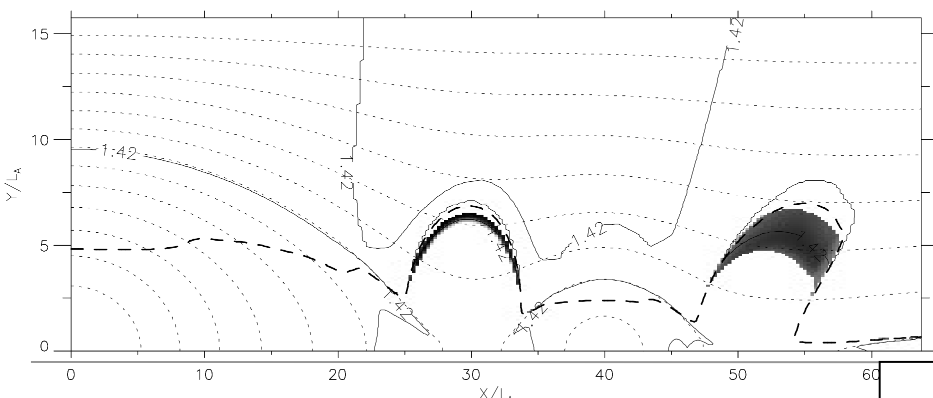

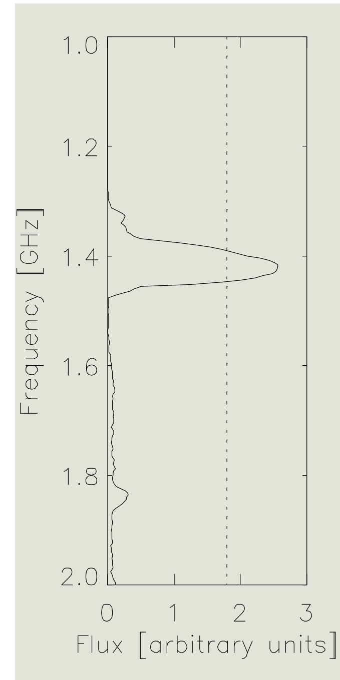

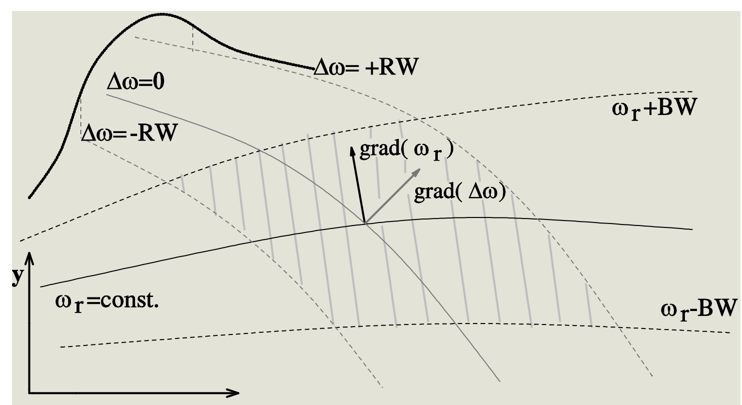

Barta & Karlicky 2005, ApJ 631

Methods of radio astronomy

Solar radio dynamic spectroscopy

Radio signatures of turbulence in the reconnection outflows

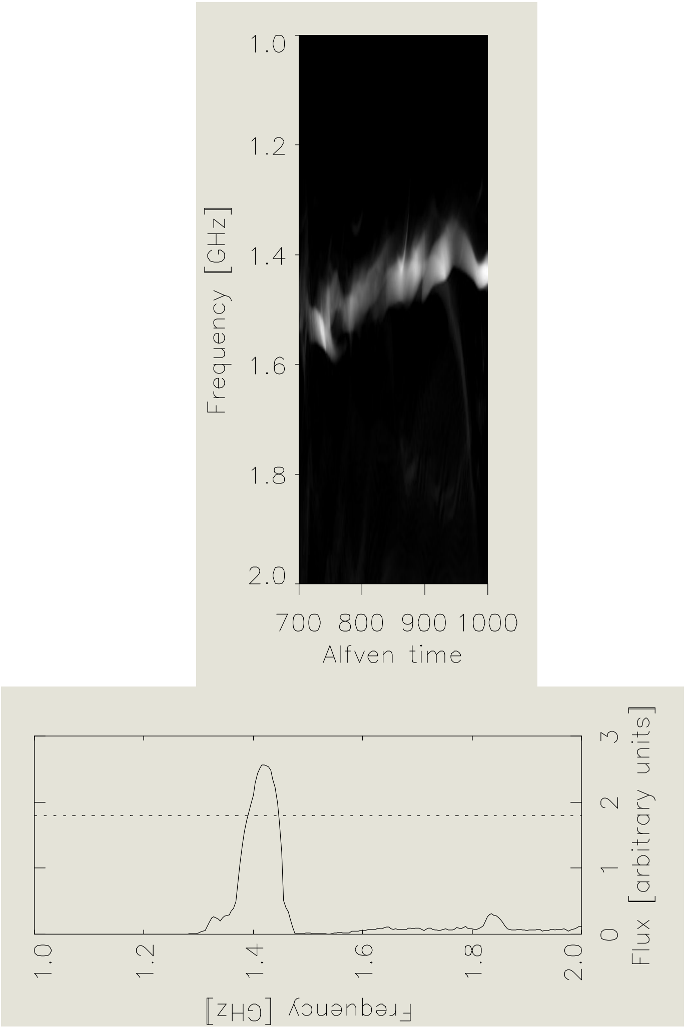

Lace burst

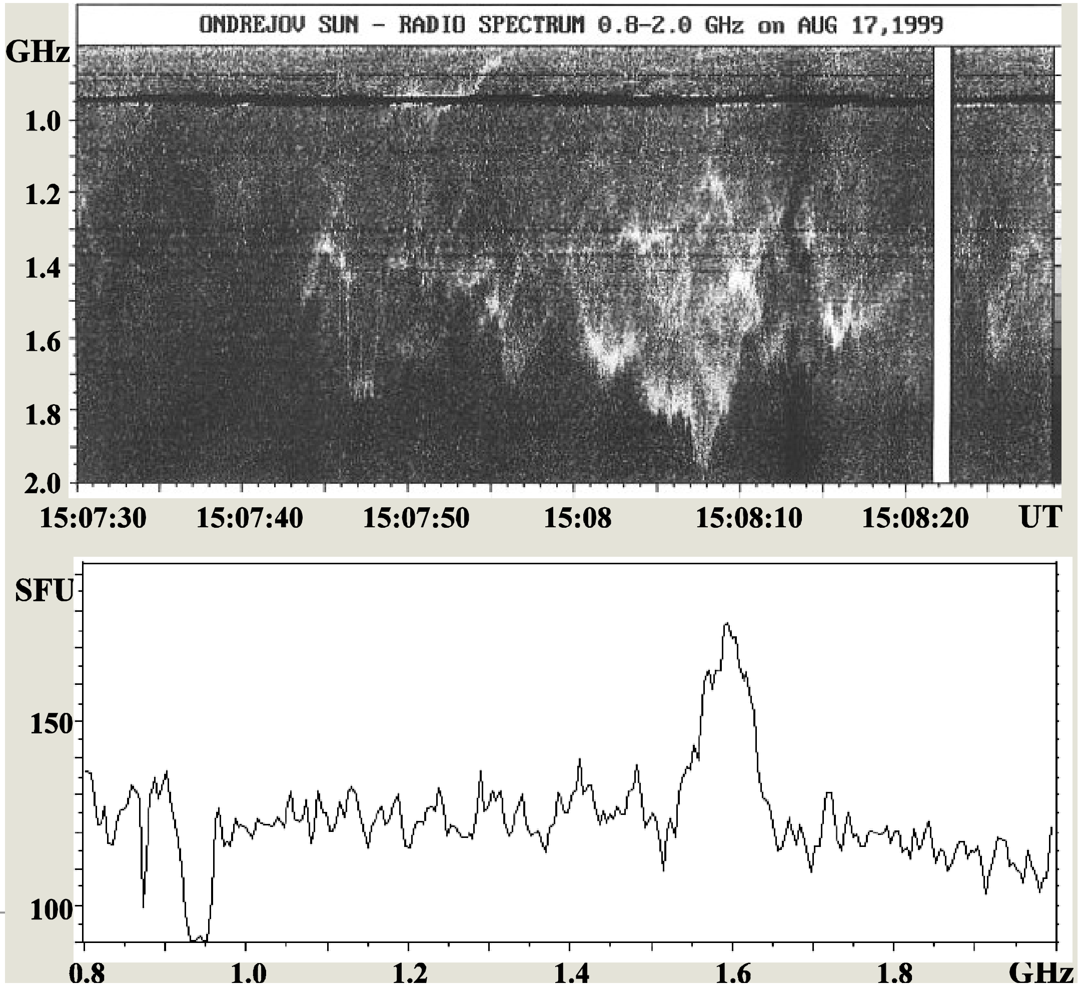

Methods of radio astronomy

Solar radio dynamic spectroscopy

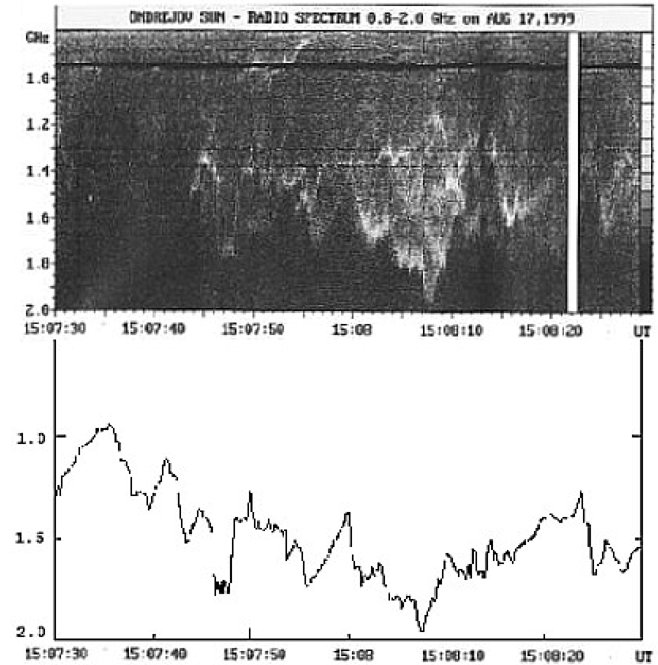

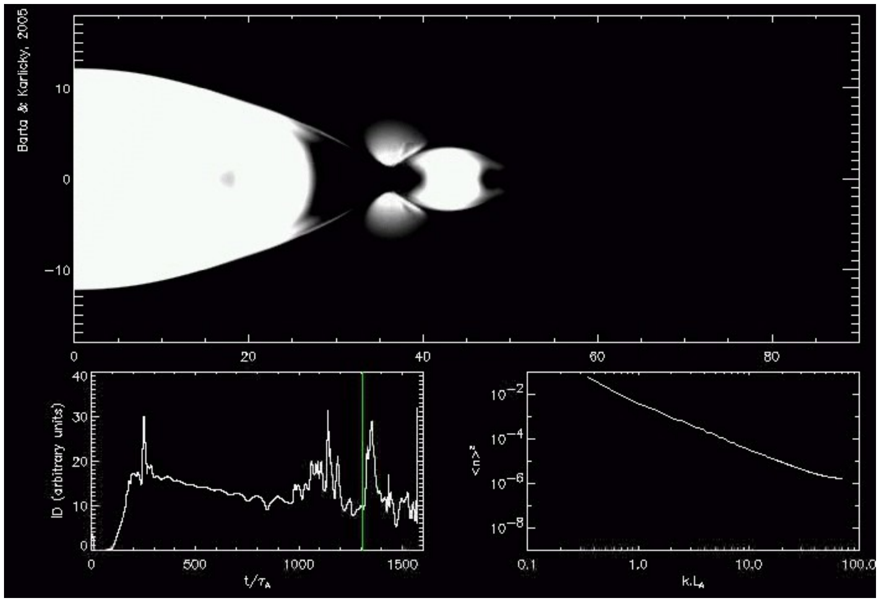

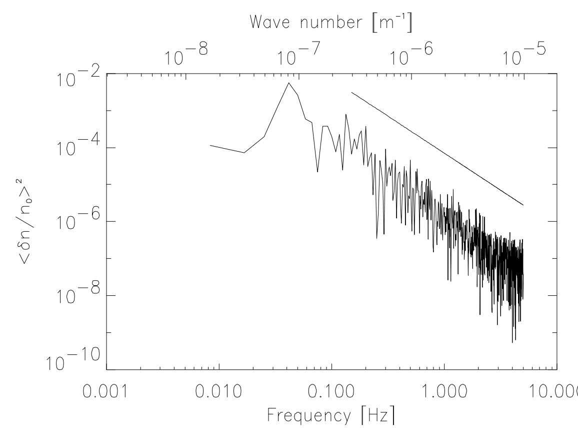

Radio signatures of turbulence in the reconnection outflows

Methods of radio astronomy

Solar radio dynamic spectroscopy

Radio signatures of turbulence in the reconnection outflows

Density fluctuations

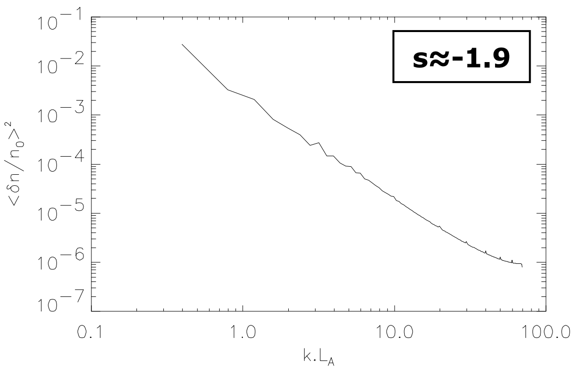

Model

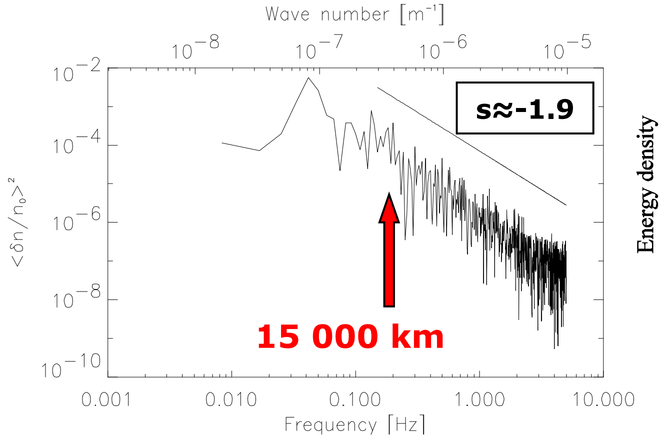

Inferred from observations (lace burst)

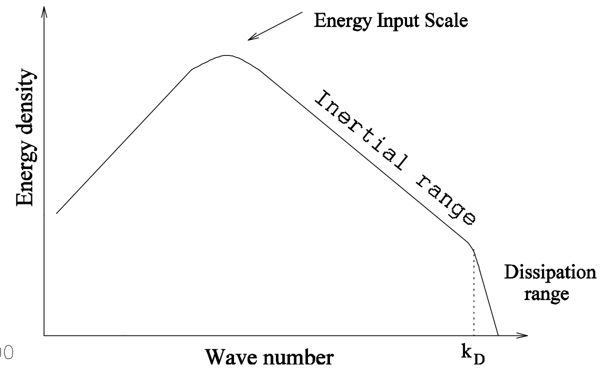

HD turbulence (scheme)

Application: Plasma turbulence diagnostics

What plasma parameters can be estimated:

1. Turbulence level in the jet
2. Energy input scale
3. Energy dissipation rate
4. Power released to kinetic energy

Radiation from turbulent reconnection jets:
Increased turbulence can interrupt emission

dm spikes

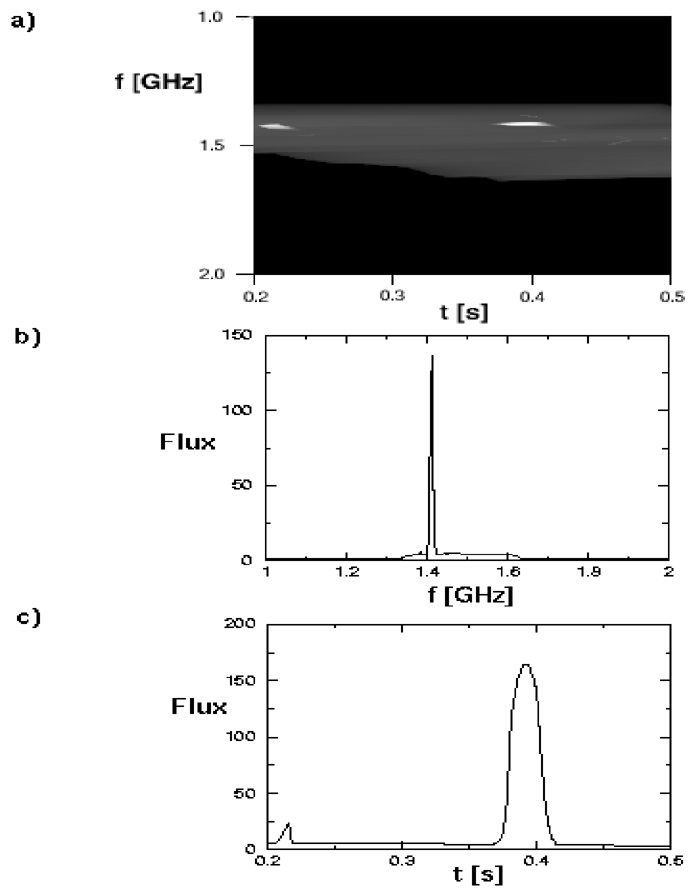

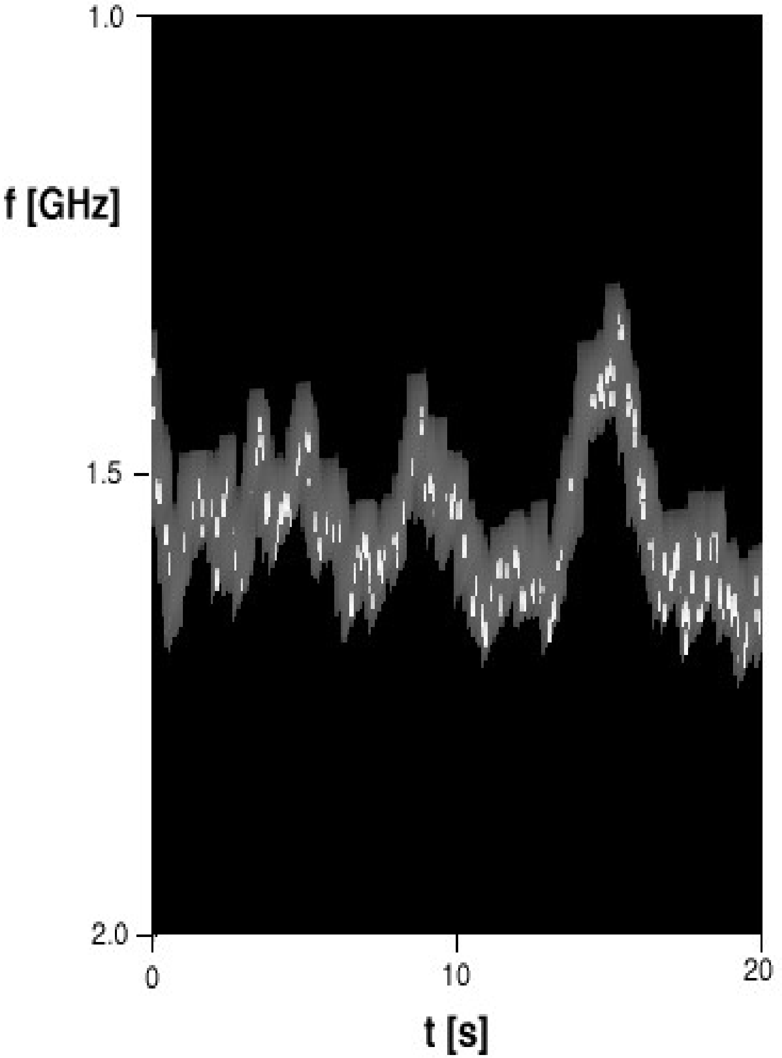

Barta & Karlicky 2001, A&A

Solar radio dynamic spectroscopy

zebra pattern

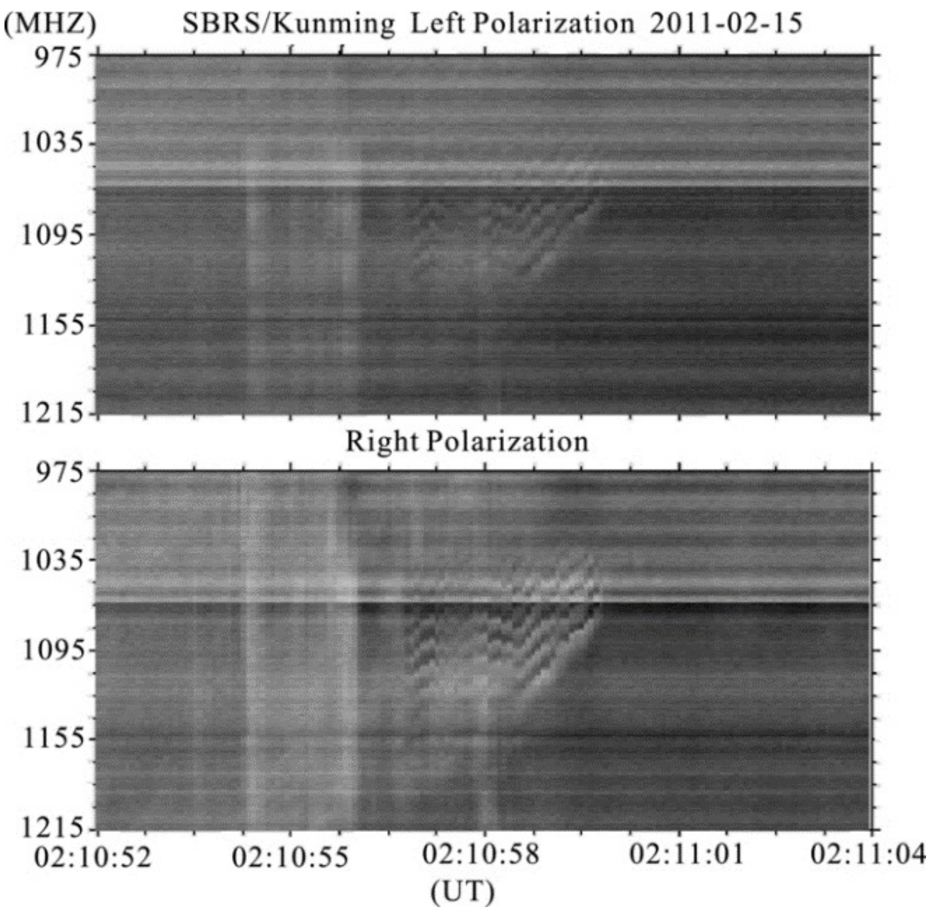

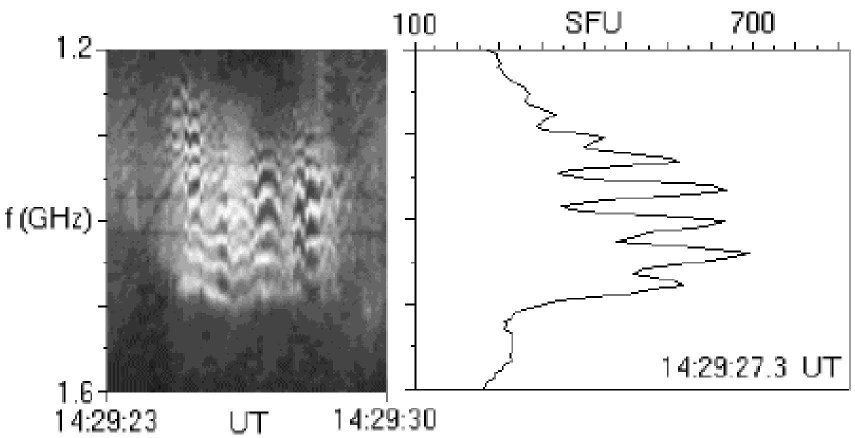

Methods of radio astronomy

Solar radio dynamic spectroscopy

Received radiation pattern is formed also by properties of interleaved plasma!

zebra pattern

$$\frac{\partial^2 \boldsymbol{E}(\boldsymbol{r},t)}{\partial t^2} - c^2 \Delta \boldsymbol{E}(\boldsymbol{r},t) + \omega_{\mathrm{p}}^2(\boldsymbol{r})\boldsymbol{E}(\boldsymbol{r},t) = 0,$$

where

$$\omega_{\mathrm{p}}^2(\boldsymbol{r}) = \frac{n(\boldsymbol{r})e^2}{\varepsilon_0 m_{\mathrm{e}}}$$

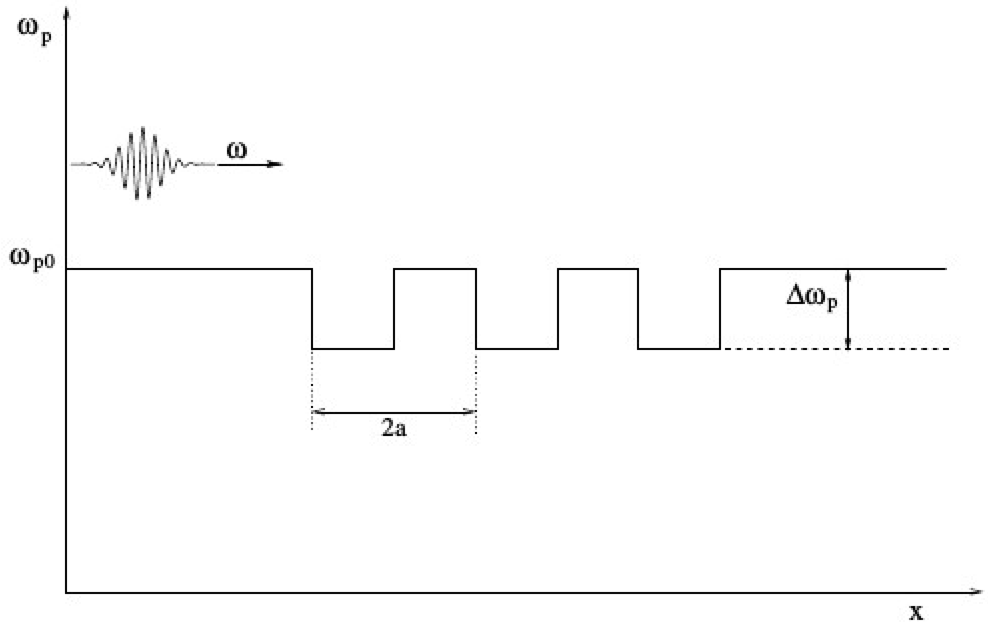

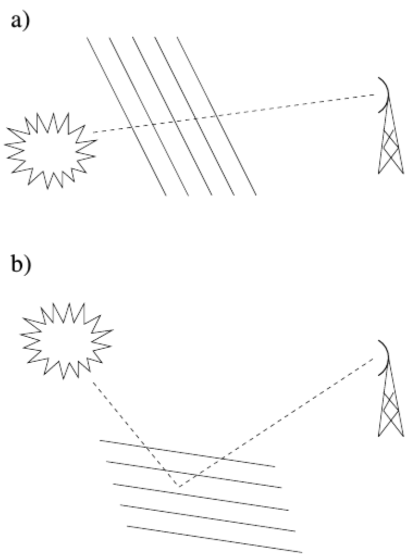

Influence of interleaved periodic structures: frequency filtering.
Similar effect to allowed/forbidden energy belts in crystals.

zebra pattern

$$\frac{\partial^2 \boldsymbol{E}(\boldsymbol{r},t)}{\partial t^2} - c^2 \triangle \boldsymbol{E}(\boldsymbol{r},t) + \omega_p^2(\boldsymbol{r}) \boldsymbol{E}(\boldsymbol{r},t) = 0,$$

where

$$\omega_p^2(\boldsymbol{r}) = \frac{n(\boldsymbol{r})e^2}{\varepsilon_0 m_e}$$

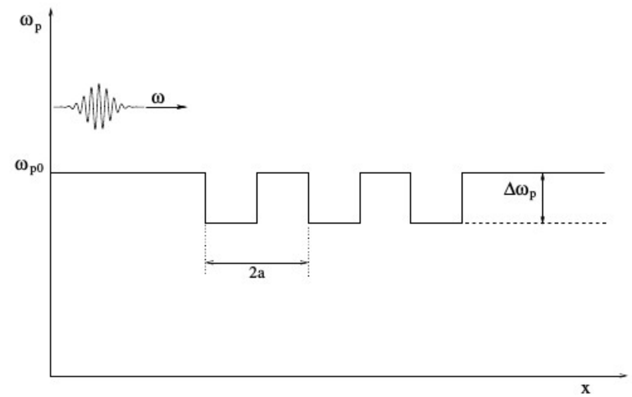

$$\omega_p(\boldsymbol{r}) = \omega_{p0} + \delta\omega_p(\boldsymbol{r}).$$

$$m = \frac{\hbar \omega_p}{c^2}.$$

$$i\hbar \frac{\partial \boldsymbol{E}}{\partial t} = -\frac{\hbar^2 \triangle}{2m_0} \boldsymbol{E} + \left(V(\boldsymbol{r}) + m_0 c^2\right) \boldsymbol{E}$$

with

$$V(\boldsymbol{r}) = \hbar\, \delta\omega_p(\boldsymbol{r}).$$

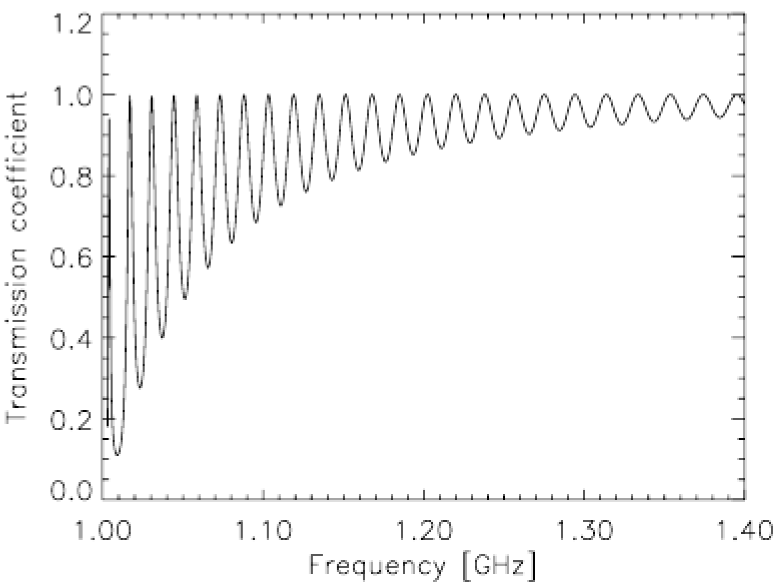

Methods of radio astronomy

Solar radio dynamic spectroscopy

Influence of interleaved periodic structures: frequency filtering.
Similar effect to allowed/forbidden energy belts in crystals.

zebra pattern

Observation

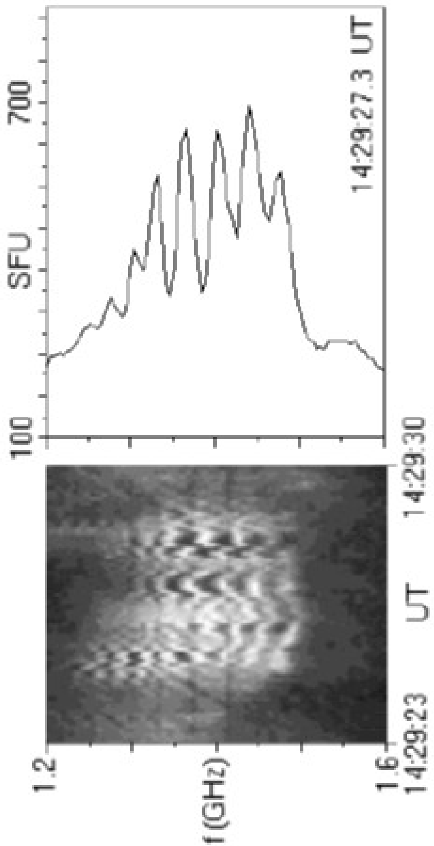

Model

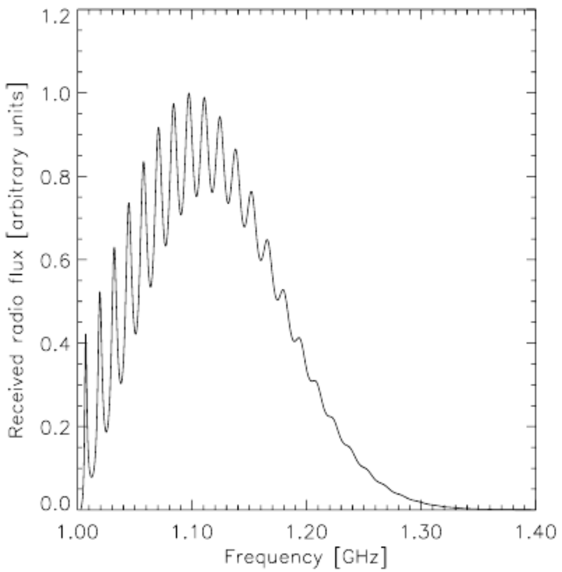

Barta & Karlicky 2006, A&A

Methods of radio astronomy

Solar radio dynamic spectroscopy

Calibration of spectral data

$$P_{rec}(f) = G(f) \cdot B(f) + P_{sys}(f)$$

Methods of calibration

- Absolute: Hot and ambient loads – noise generators (heated resistors noise diode, …)
- Relative: Scaled to an (celestial) object with known radio brightness – *calibrator*
  Typical radio flux calibrators: Quasars, solar system objects (planets & their moons)

For spectroscopic data all quantities are frequency dependent.
Finding $G=G(f)$ and $T_{sys}=T_{sys}(f)$ from observed calibrators with known spectrum
→ **bandpass calibration**

For dynamic radio spectra of solar bursts the *Quiet Sun Radiation* (QSR) with well known spectral properties is used as calibrator:

$$G(f) = \frac{P_{obs}^{QSR}(f) - N(f)}{P_{teor}^{QSR}(f)} \quad \longrightarrow \quad F_{cal}(f) = \frac{QSR_{teor}(f)}{QSR_{meas}(f) - N(f)} \cdot [F_{meas}(f) - N(f)]$$

Methods of radio astronomy

Solar radio dynamic spectroscopy

Calibration of spectral data

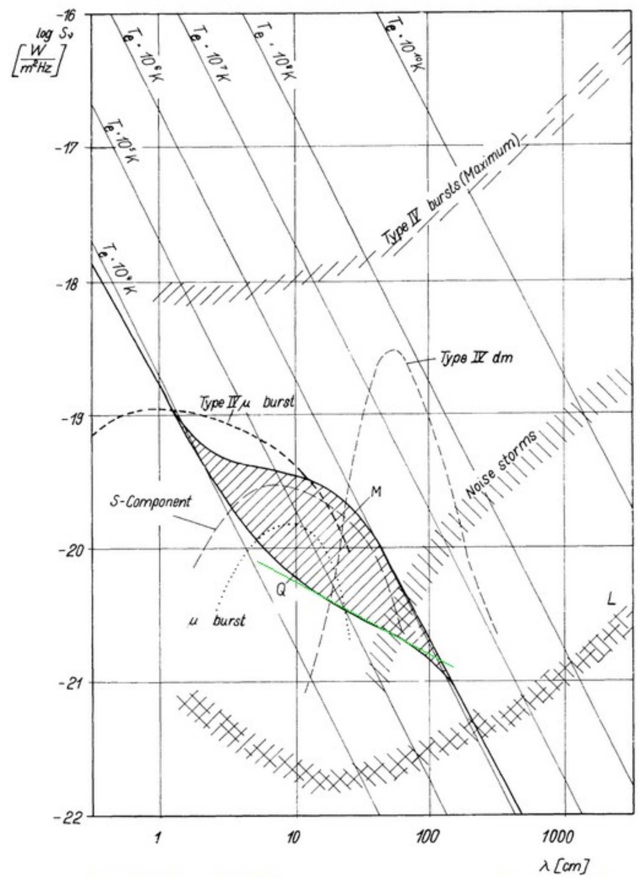

Fig. III.1. Solar radio spectra: Q – 'quiet Sun', M – maximum daily flux; L – limit of detectability of single-frequency patrol observations (after Krüger, 1968).

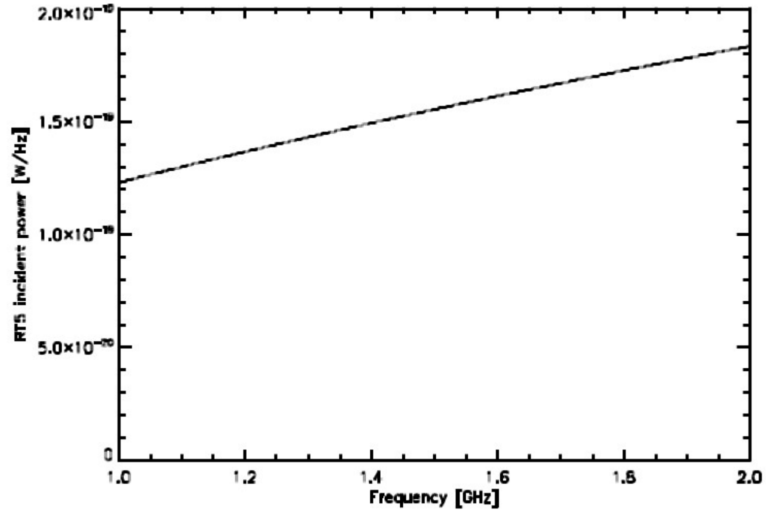

$$\frac{P_{QSR\ Inc}(f)}{W\ Hz^{-1}} = 1{,}23\times10^{-19}\cdot\left(\frac{f}{GHz}\right)^{0{,}577}$$

$$F_{cal}(f)=\frac{QSR_{teor}(f)}{QSR_{meas}(f)-N(f)}\cdot[F_{meas}(f)-N(f)]$$

Methods of radio astronomy

Solar radio dynamic spectroscopy

Calibration of spectral data

Uncalibrated data

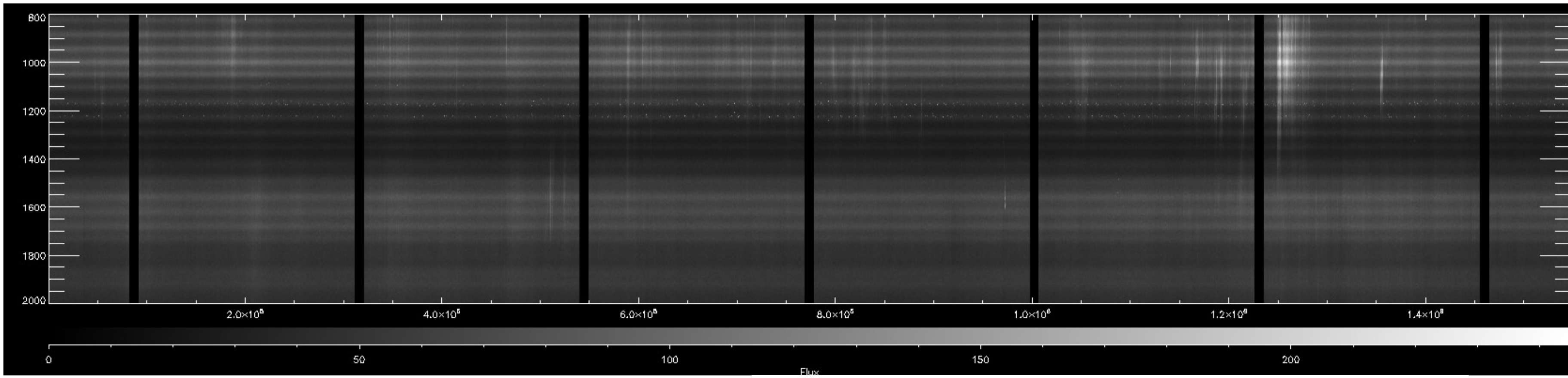

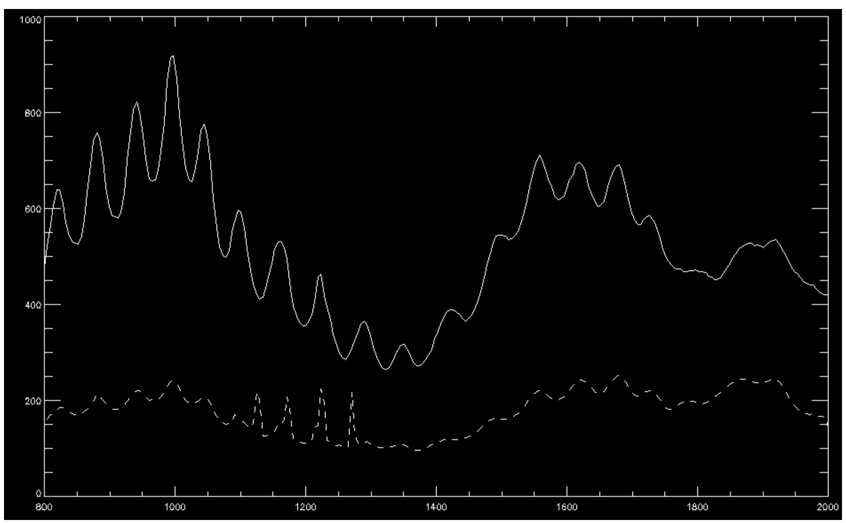

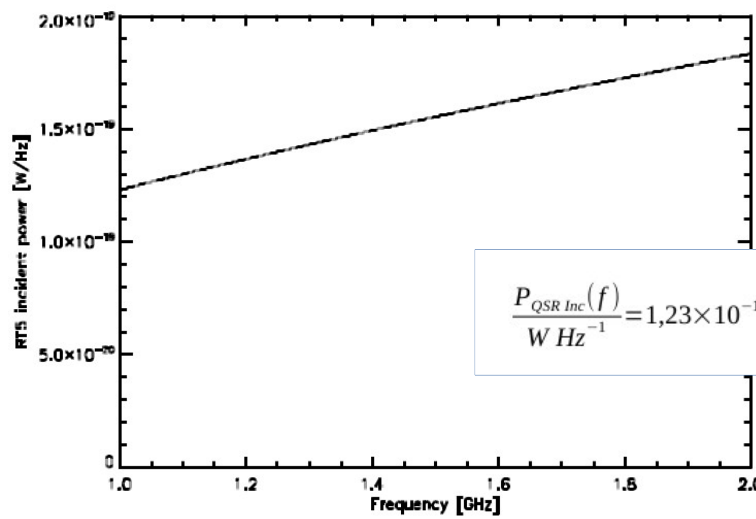

$$\frac{P_{QSR\ Inc}(f)}{W\ Hz^{-1}} = 1{,}23 \times 10^{-19} \cdot \left(\frac{f}{GHz}\right)^{0{,}577}$$

Methods of radio astronomy

Solar radio dynamic spectroscopy

Calibration of spectral data

Calibrated data

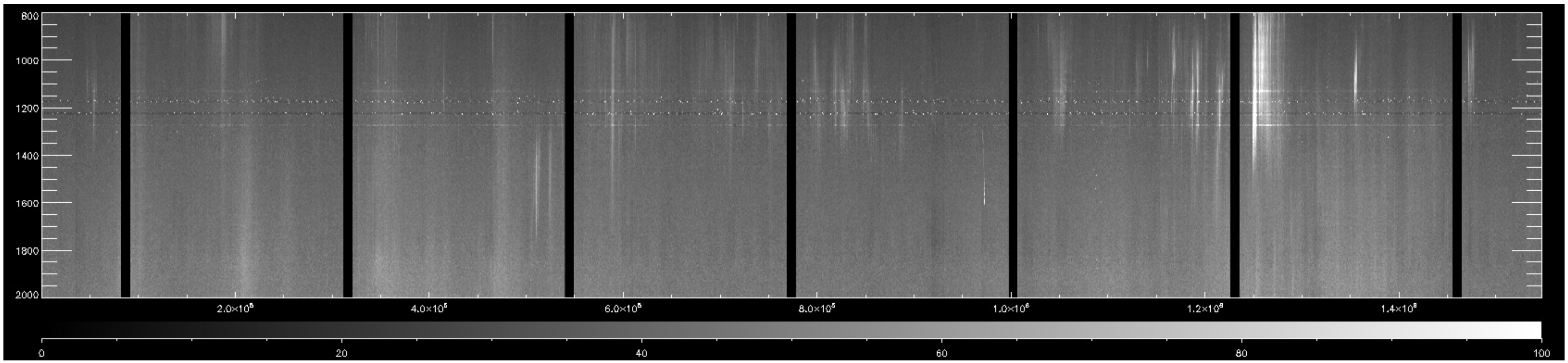

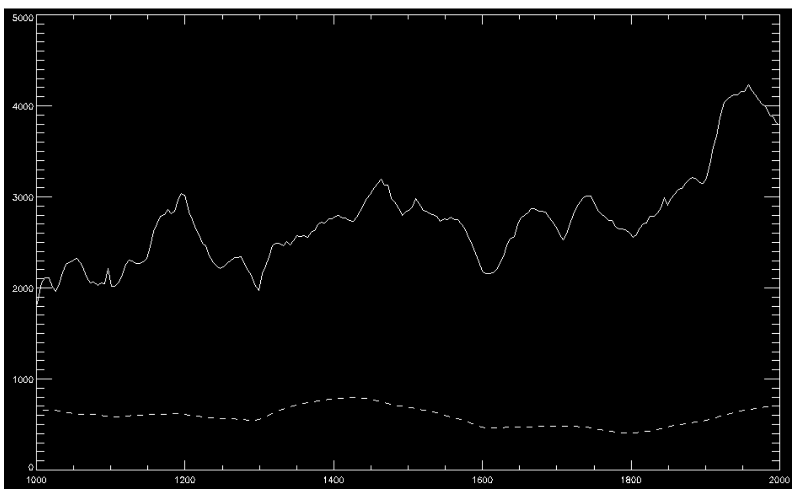

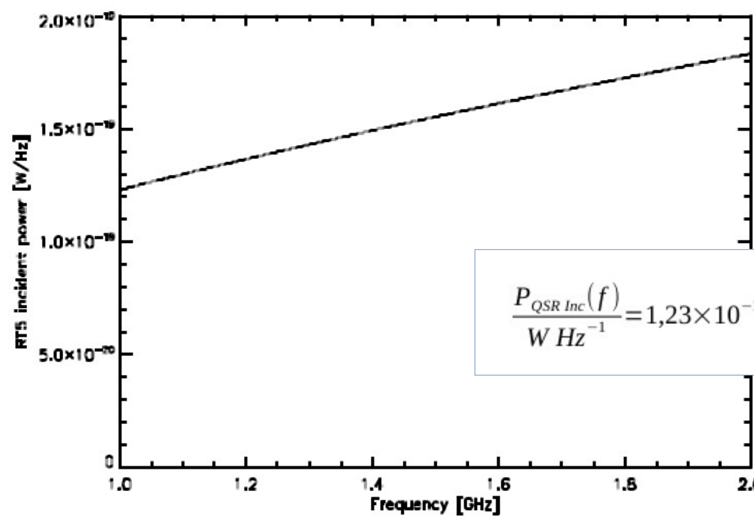

$$\frac{P_{QSR\ Inc}(f)}{W\ Hz^{-1}} = 1{,}23\times10^{-19}\cdot\left(\frac{f}{GHz}\right)^{0{,}577}$$

Methods of radio astronomy

Radio dynamic spectroscopy / spectropolarimetry: Non-solar applications

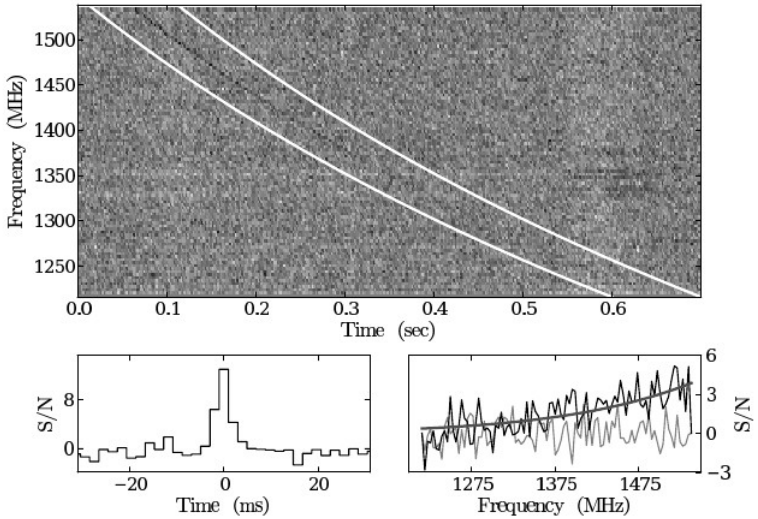

Figure 2. Characteristic plots of FRB 121102. In each panel the data were smoothed in time and frequency by a factor of 30 and 10, respectively. The top panel is a dynamic spectrum of the discovery observation showing the 0.7 s during which FRB 121102 swept across the frequency band. The signal is seen to become significantly dimmer towards the lower part of the band, and some artifacts due to RFI are also visible. The two white curves show the expected sweep for a ν^{-2} dispersed signal at a DM = 557.4 pc cm^{-3}. The lower left panel shows the dedispersed pulse profile averaged across the bandpass. The lower right panel compares the on-pulse spectrum (black) with an off-pulse spectrum (light gray), and for reference a curve showing the fitted spectral index ($\alpha = 10$) is also overplotted (medium gray). The on-pulse spectrum was calculated by extracting the frequency channels in the dedispersed data corresponding to the peak in the pulse profile. The off-pulse spectrum is the extracted frequency channels for a time bin manually chosen to be far from the pulse.

Fast Radio Bursts / FRBs

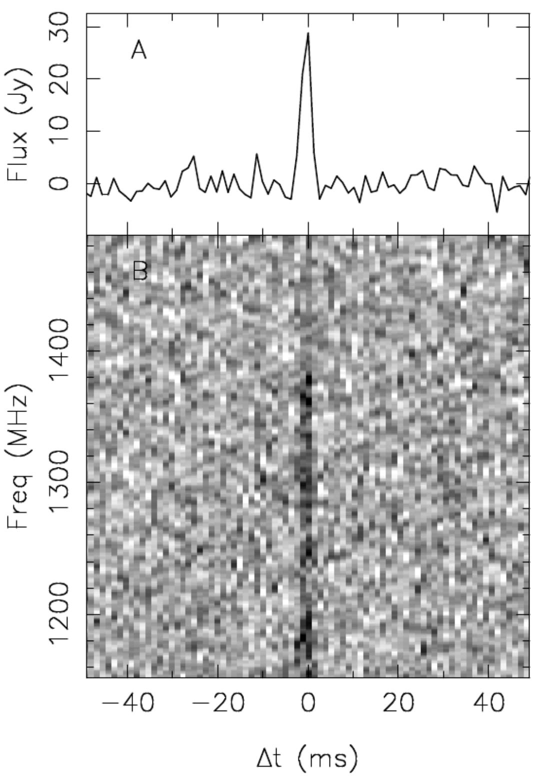

FRB.gif

Methods of radio astronomy

Radio dynamic spectroscopy / spectropolarimetry: Non-solar applications

Fast Radio Bursts / FRBs

$$\omega^2 = \omega_{pe}^2 + k^2 c^2$$

$$v_g = \frac{\partial \omega}{\partial k}$$

$$v_g = c\sqrt{1 - \frac{\omega_p^2}{\omega^2}}$$

$$\frac{1}{v_g} = \frac{1}{c}\left(1 + \frac{1}{2}\frac{\nu_p^2}{\nu^2}\right)$$

$$\tau_D = \int_0^L \frac{dl}{v_g} \cong \frac{1}{c}\int_0^L \left(1 + \frac{1}{2}\left(\frac{\nu_p}{\nu}\right)^2\right) dl = \frac{1}{c}\int_0^L \left(1 + \frac{e^2}{2\pi m_e}\frac{1}{\nu^2}N(l)\right) dl$$

$$\tau_D = \frac{L}{c} + \frac{e^2}{2\pi c\, m_e}\frac{1}{\nu^2}\int_0^L N(l)\, dl\,.$$

$$\Delta\tau_D = \frac{e^2}{2\pi c\, m_e}\left[\frac{1}{\nu_1^2} - \frac{1}{\nu_2^2}\right]\int_0^L N(l)\, dl$$

Radio dynamic spectroscopy / spectropolarimetry: Non-solar applications

$$\Delta \tau_{\mathrm{D}} = \frac{e^2}{2\pi c\, m_{\mathrm{e}}} \left[\frac{1}{\nu_1^2} - \frac{1}{\nu_2^2} \right] \int_0^L N(l)\, \mathrm{d}l$$

$$\mathrm{DM} = \int_0^\infty \left(\frac{N}{\mathrm{cm}^{-3}} \right) \mathrm{d} \left(\frac{l}{\mathrm{pc}} \right)$$

Dispersion measure

Fast Radio Bursts / FRBs

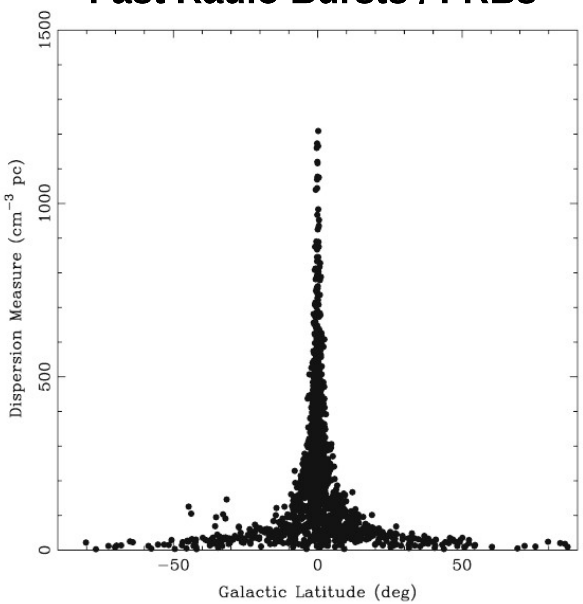

Fig. 2.3 Dispersion measure, DM, for pulsars at different galactic latitudes [adapted from B. Klein (MPIfR) unpublished]

Radio dynamic spectroscopy / spectropolarimetry: Non-solar applications

$$\Delta \tau_D = \frac{e^2}{2\pi c m_e} \left[\frac{1}{\nu_1^2} - \frac{1}{\nu_2^2} \right] \int_0^L N(l)\, dl$$

$$\mathrm{DM} = \int_0^\infty \left(\frac{N}{\mathrm{cm}^{-3}} \right) \mathrm{d} \left(\frac{l}{\mathrm{pc}} \right)$$

Fast Radio Bursts / FRBs

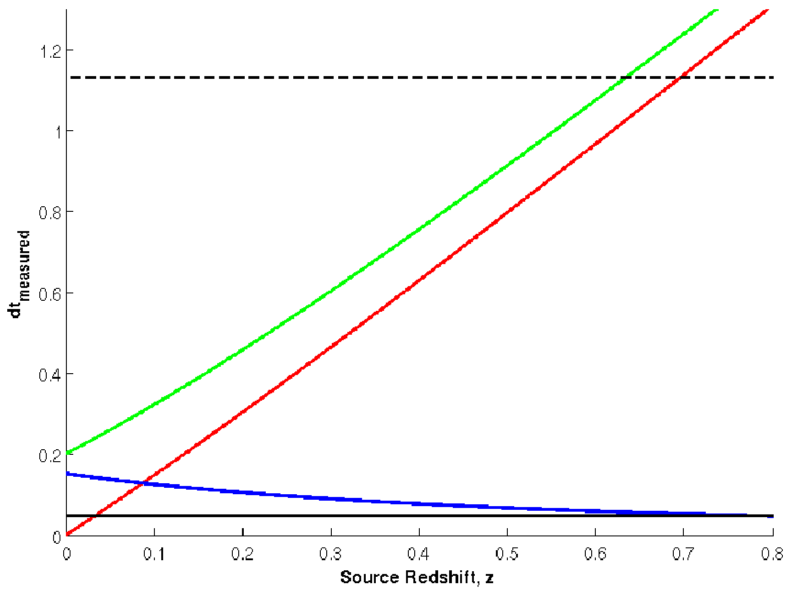

Figure 5.4 – Modelled dispersive delay (in seconds) across the observing band of the HTRU survey is shown plotted against redshift. The flat dashed line indicates the delay across the observing band for FRB 110220. The solid black line is the MW contribution and is constant irrespective of the redshift of the source, the red line is the delay due to the IGM, the blue line is the delay contribution from a host galaxy with $\mathrm{DM_{Host}} = 100\ \mathrm{cm^{-3}pc}$, and the green line is the sum of the IGM, host and MW contributions. When the sum of contributions is equal to the measured delay the redshift is inferred.

Radio dynamic spectroscopy / spectropolarimetry: Non-solar applications

Weird signal @ Arecibo (Astropis 2017/2)

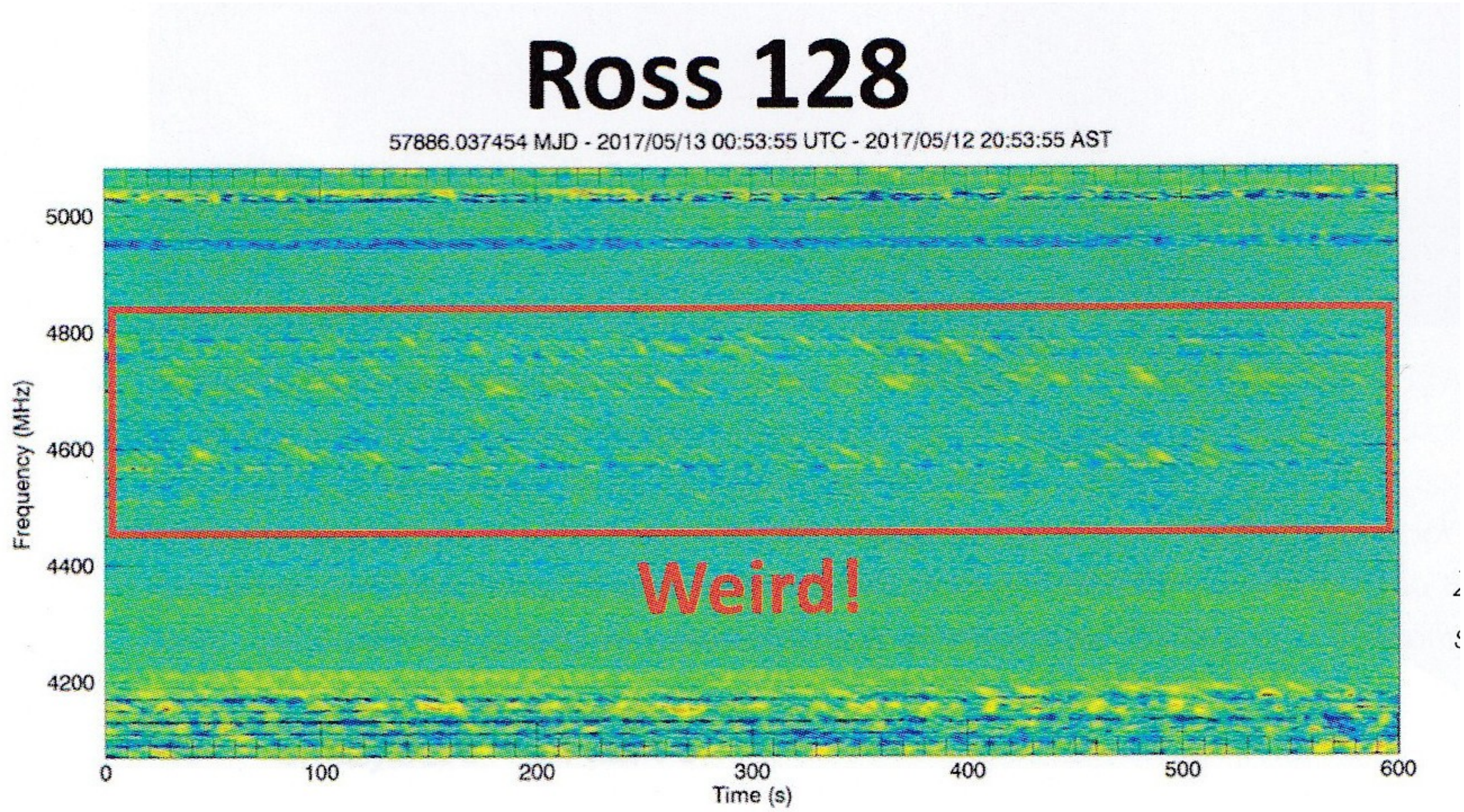

Radio dynamic spectroscopy / **spectropolarimetry**: Non-solar applications

Faraday rotation

$$k_{\pm}^2 = \frac{\omega^2}{c^2}\left(1 - \frac{\omega_p^2}{\omega(\omega \pm \omega_c)}\right)$$

Ordinary/extraordinary ELMG wave in magnetised plasma

$$2\Delta\psi = (k_+ - k_-)\Delta z$$

$$\Delta\psi = \frac{\omega_p^2\omega_c}{2c\,\omega^2}\Delta z = \frac{2\pi N e^3 B}{m^2 c\,\omega^2}\Delta z$$

$$\Delta\psi = \frac{e^3}{2\pi m^2 c}\frac{1}{\nu^2}\int_0^L B_{\parallel}(z) N(z)\,\mathrm{d}z$$

$$\frac{\mathrm{RM}}{\mathrm{rad\,m^{-2}}} = 8.1\times10^5 \int_0^{L/\mathrm{pc}} \left(\frac{B_{\parallel}}{\mathrm{Gauss}}\right)\left(\frac{N_e}{\mathrm{cm^{-3}}}\right)\mathrm{d}\left(\frac{z}{\mathrm{pc}}\right) = \frac{\left(\frac{\Delta\psi_1}{\mathrm{rad}}\right) - \left(\frac{\Delta\psi_2}{\mathrm{rad}}\right)}{\left(\frac{\lambda_1}{\mathrm{m}}\right)^2 - \left(\frac{\lambda_2}{\mathrm{m}}\right)^2}$$

Overview on interferometry
(main lecture next time)

“Old-fashion” radio interferometry: Phased arrays - **analog signal sum**

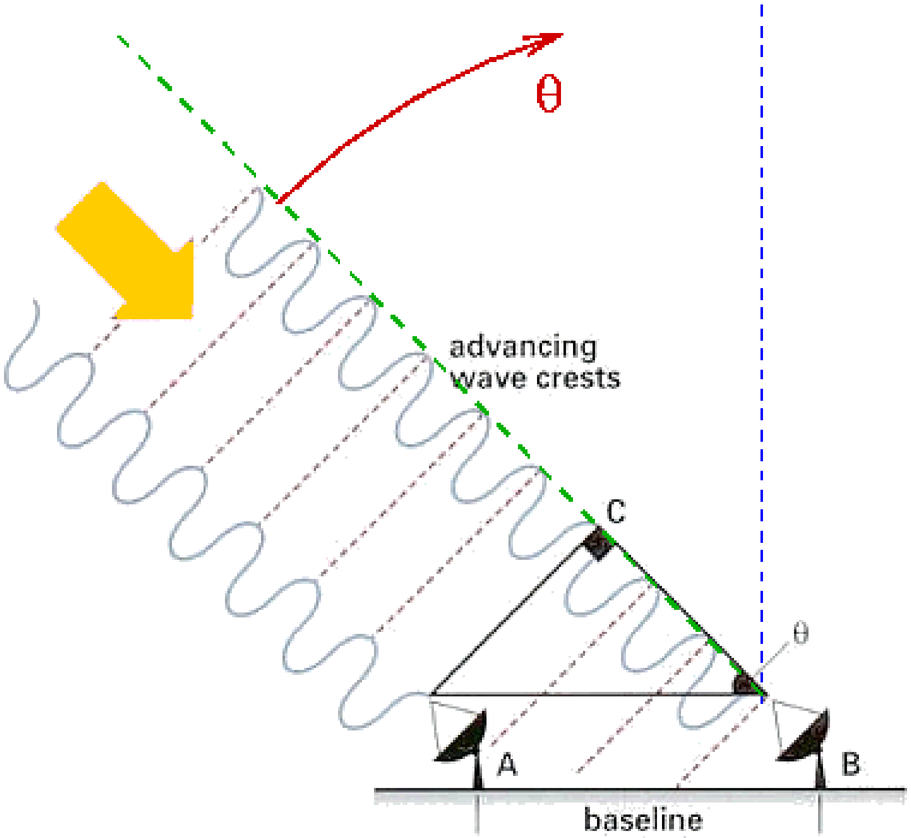

Known result from
a **double-slit experiment**:

$$|I_{AB}(\theta)| = 1 + \cos\frac{2\pi D}{\lambda}\theta$$

"Old-fashion" radio interferometry: Phased arrays - **analog signal sum**

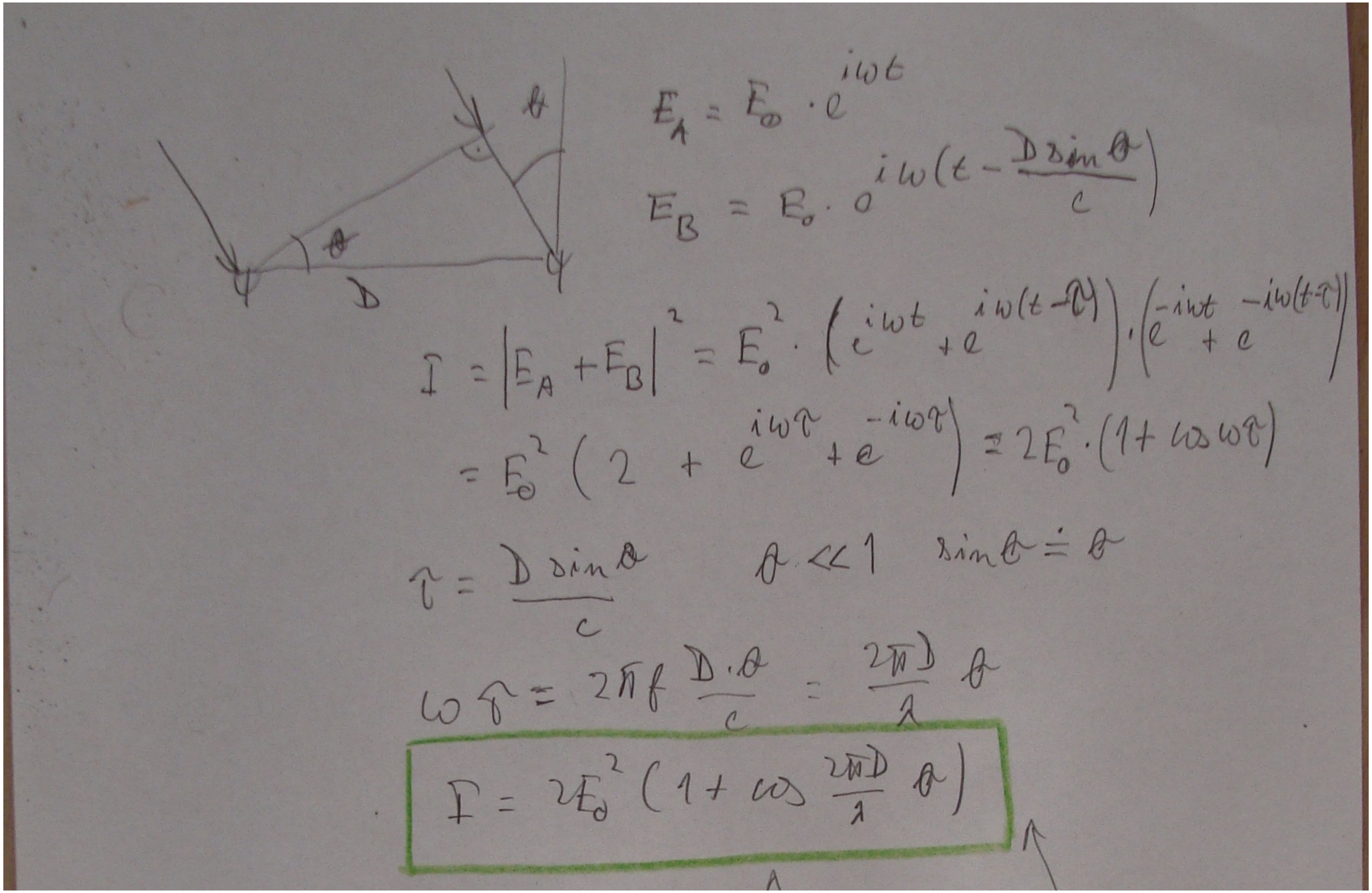

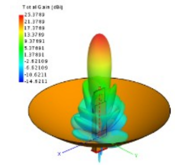

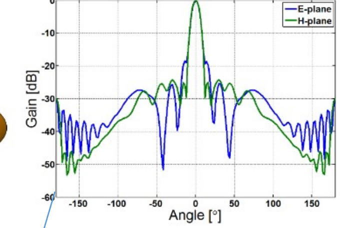

Old good times – **sparse antenna rows / phased arrays** (beam forming)

Analogy with **optical gratings** used in spectrographs

$$|I_{\Sigma}(\theta)| = \frac{1 - \cos N \frac{2\pi D}{\lambda}\theta}{1 - \cos \frac{2\pi D}{\lambda}\theta}$$

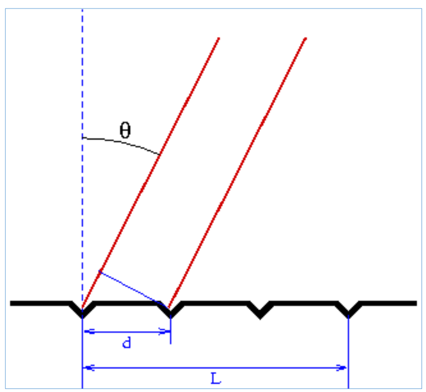

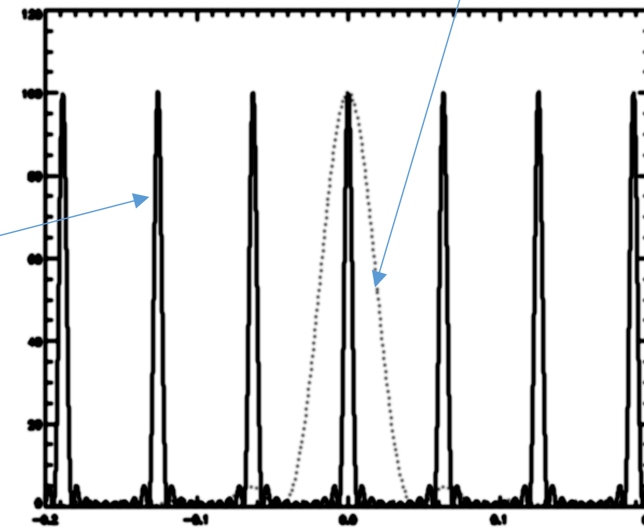

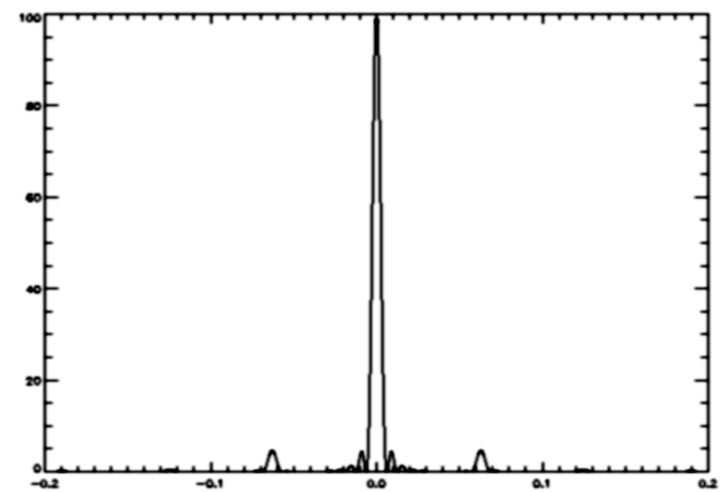

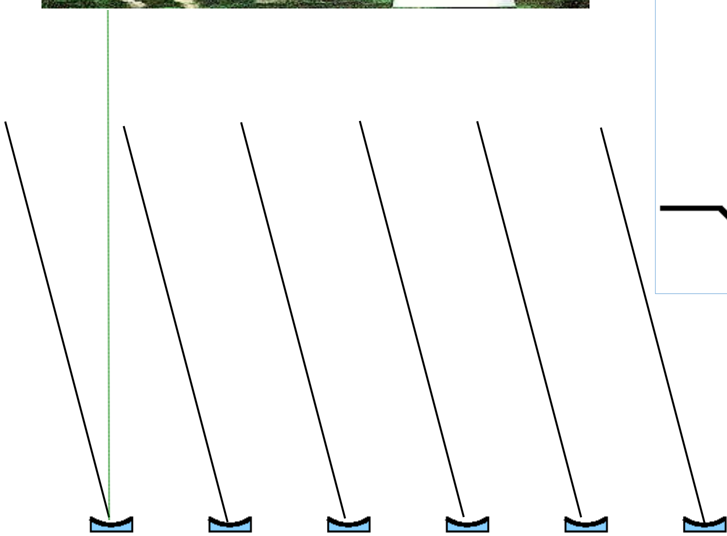

Methods of radio astronomy

"Old-fashion" radio interferometry: Phased arrays - **analog signal sum**

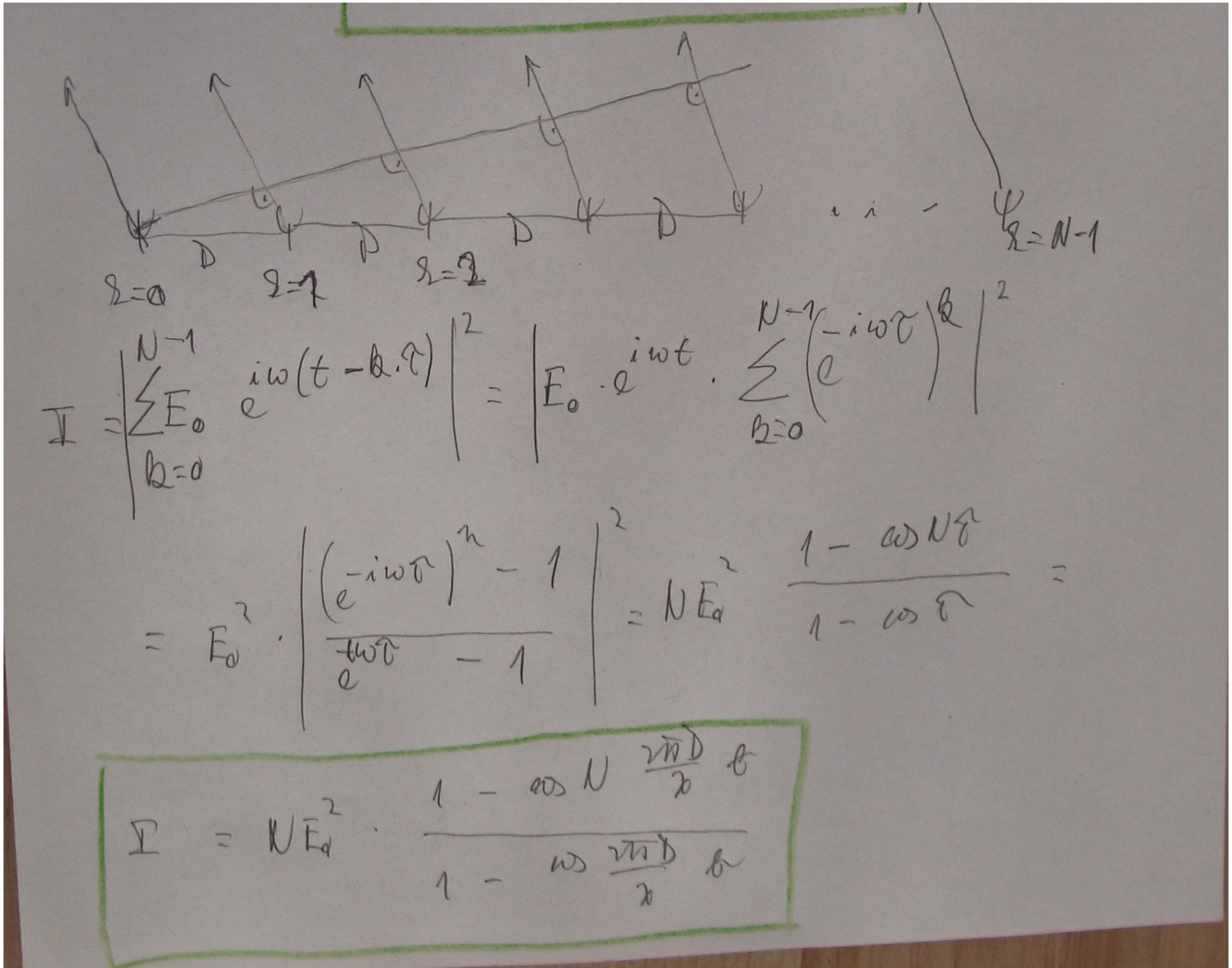

Old good times – **sparse antenna rows/ phased arrays**

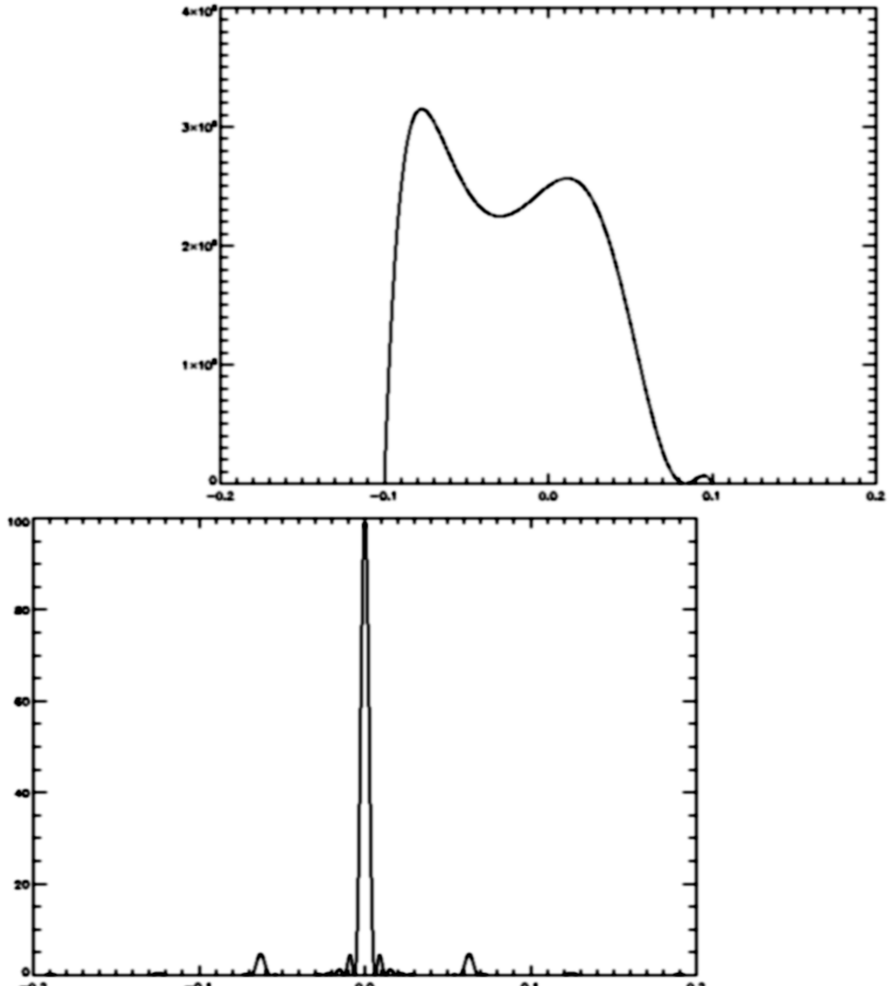

- Scanning with the beam
- Frequently supplied by MFI

Methods of radio astronomy

Modern systems - **digital signal product**

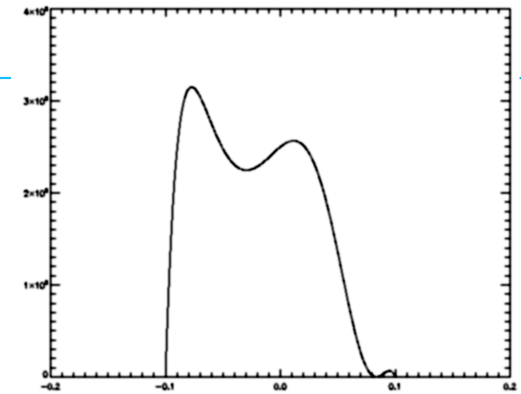

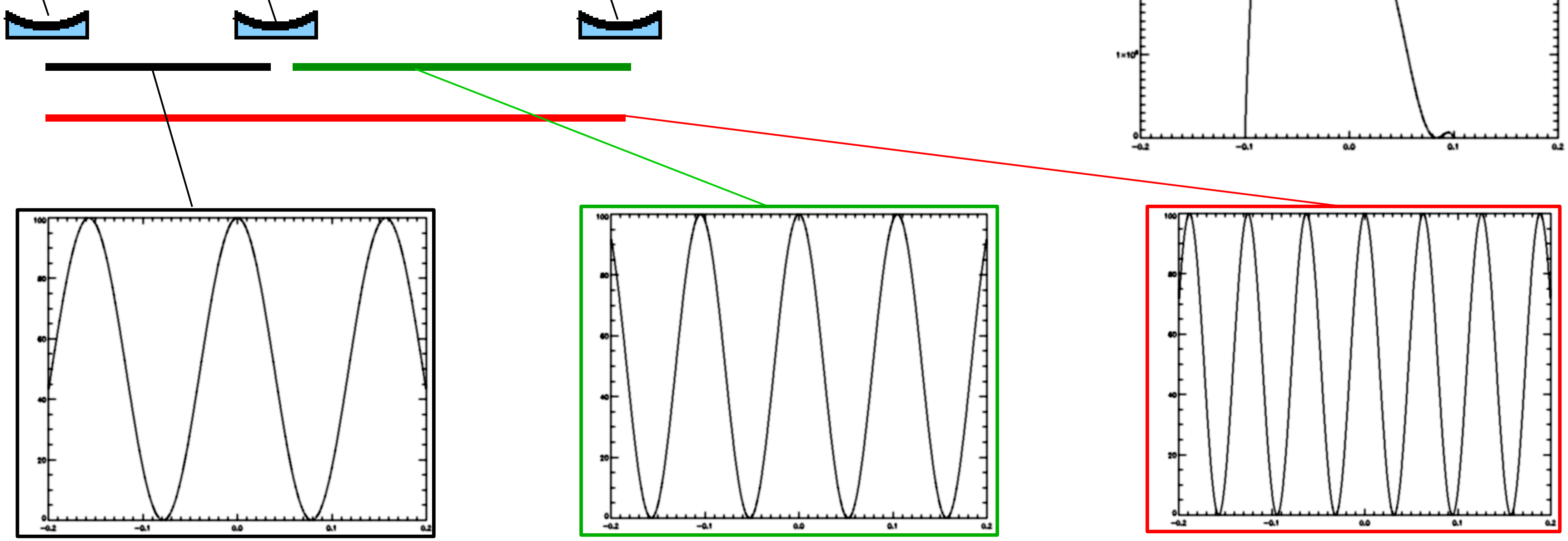

Nowadays: Aperture synthesis – decomposition of image to harmonics = Fourier transform

$$\langle P_{12}(D/\lambda)\rangle = \langle E_1 . \overline{E_2}\rangle = G \cdot \int_{-\infty}^{+\infty} B(\theta) \exp\left(i \frac{2\pi D}{\lambda}\theta\right) d\theta$$

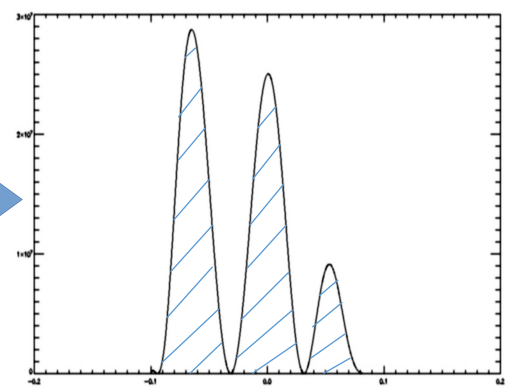

Cross-correlations → **interferometric visibilities**

Radio interferometry / aperture synthesis

$$\langle I_{AB}\rangle(\theta) = \int_{-\infty}^{+\infty} B(\theta)\, \exp\left(i\frac{2\pi D}{\lambda}\theta\right) d\theta$$

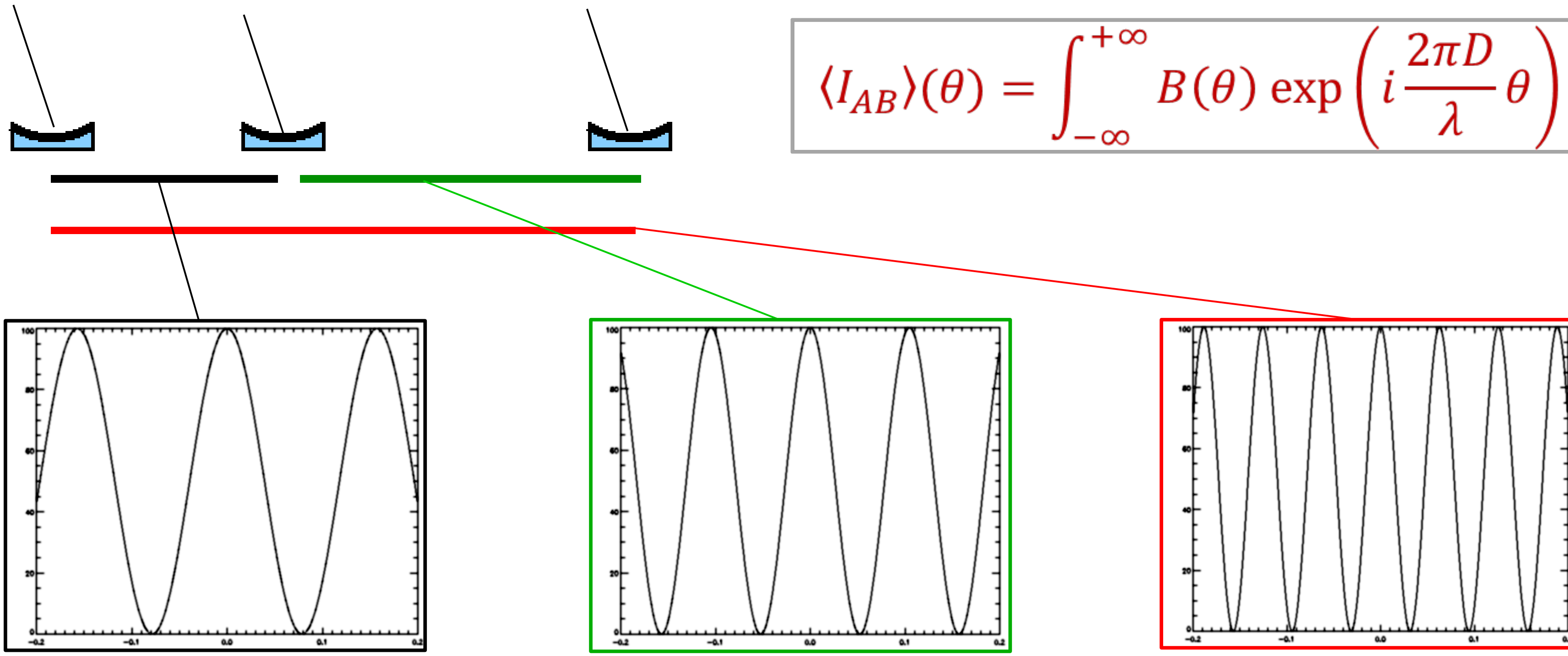

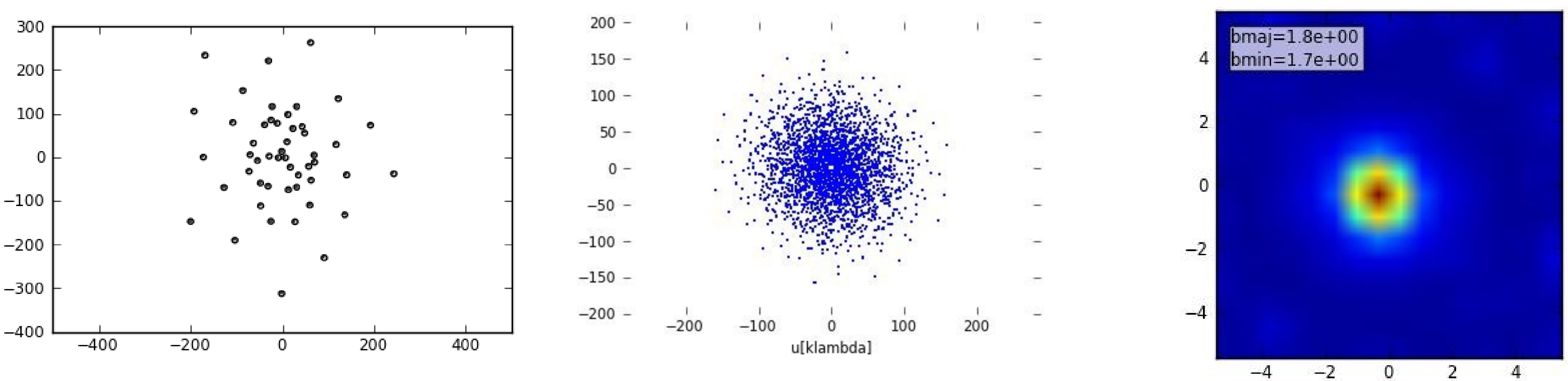

Methods of radio astronomy

Radio interferometry / aperture synthesis

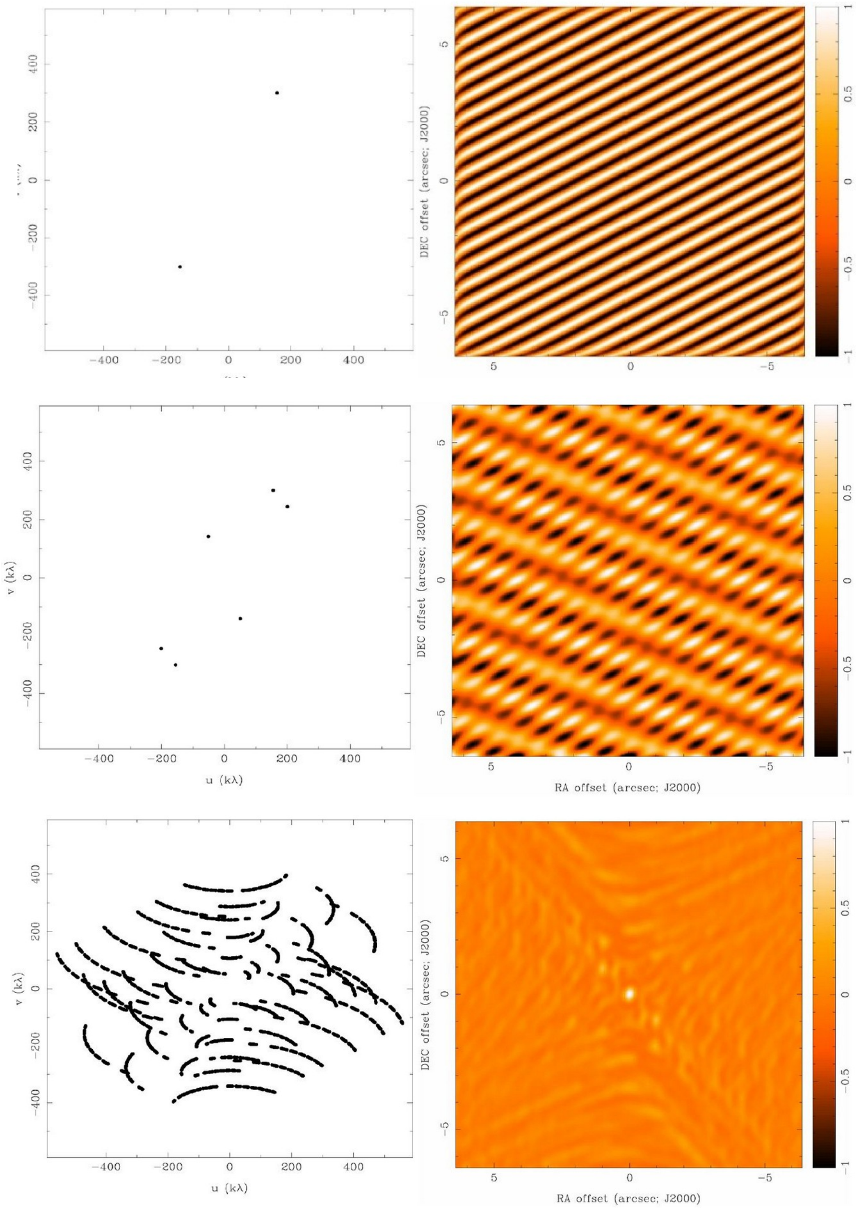

Response to the point source

2 antennas

3 antennas

8 antennas x 240 samples

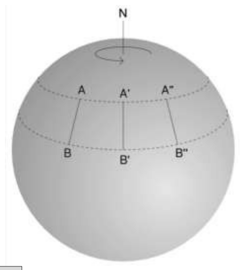

Much more comes in the next lecture!